Article

sp Carbon Chains Surrounded by sp Carbon Double Helices: Coordination-Driven Self-Assembly of Wirelike Pt(C#C)Pt Moieties That Are Spanned by Two P(CH)P Linkages

Jrgen Stahl, Wolfgang Mohr, Laura de Quadras, Thomas B. Peters, James C. Bohling, Jos Miguel Martn-Alvarez, Gareth R. Owen, Frank Hampel, and John A. Gladysz

J. Am. Chem. Soc., **2007**, 129 (26), 8282-8295• DOI: 10.1021/ja0716103 • Publication Date (Web): 13 June 2007

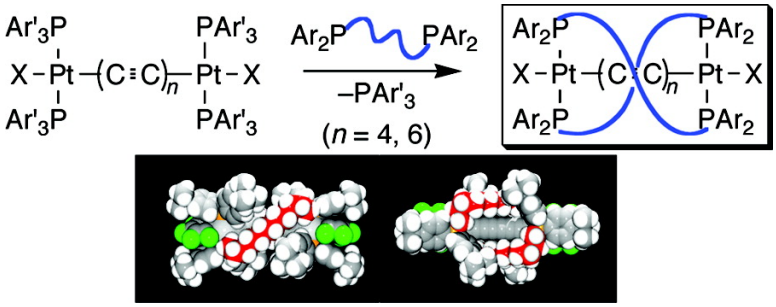

More About This Article

Additional resources and features associated with this article are available within the HTML version:

- Supporting Information
- Links to the 11 articles that cite this article, as of the time of this article download
- Access to high resolution figures
- Links to articles and content related to this article
- Copyright permission to reproduce figures and/or text from this article

View the Full Text HTML

J|A|C|S
ARTICLES
Published on Web 06/13/2007

sp Carbon Chains Surrounded by sp^3 Carbon Double Helices: Coordination-Driven Self-Assembly of Wirelike $Pt(C{\equiv}C)_nPt$ Moieties That Are Spanned by Two $P(CH_2)_mP$ Linkages

Jürgen Stahl,[†] Wolfgang Mohr,[†] Laura de Quadras,[†] Thomas B. Peters,[‡] James C. Bohling,[‡] José Miguel Martín-Alvarez,[‡] Gareth R. Owen,[†] Frank Hampel,[†] and John A. Gladysz*[,†]

Contribution from the Institut für Organische Chemie and Interdisciplinary Center for Molecular Materials, Friedrich-Alexander-Universität Erlangen-Nürnberg, Henkestraße 42, 91054 Erlangen, Germany, and Department of Chemistry, University of Utah, Salt Lake City, Utah 84112

Received March 13, 2007; E-mail: gladysz@chemie.uni-erlangen.de

Abstract: Reactions of *trans*,*trans*-$(C_6F_5)(p\text{-}tol_3P)_2Pt(C{\equiv}C)_4Pt(Pp\text{-}tol_3)_2(C_6F_5)$ and diphosphines $Ar_2P(CH_2)_m$-PAr_2 yield *trans*,*trans*-$(C_6F_5)(Ar_2P(CH_2)_mPAr_2)Pt(C{\equiv}C)_4Pt(Ar_2P(CH_2)_mPAr_2)(C_6F_5)$, in which the platinum atoms are spanned via an sp and two sp^3 carbon chains (Ar/m = **3**, Ph/14, 87%; **4**, *p*-tol/14, 91%; **5**, $p\text{-}C_6H_4\text{-}t\text{-}Bu$/14, 77%; **7**, Ph/10, 80%; **8**, Ph/11, 80%; **9**, Ph/12, 36%; only oligomers form for m > 14). Crystal structures of **3**−**5** show that the sp^3 chains adopt chiral double-helical conformations that shield the sp chain at approximately the van der Waals distance, with both enantiomers in the unit cell. The platinum square planes define angles of 196.6°−189.9° or more than a half twist. Crystal structures of **7**−**9**, which have shorter sp^3 chains, exhibit nonhelical conformations. Reaction of the corresponding $Pt(C{\equiv}C)_6Pt$ complex and $Ph_2P(CH_2)_{18}PPh_2$ gives an analogous adduct (27%). The crystal structure shows two independent molecules, one helical and the other not. Low-temperature NMR data suggest that the enantiomeric helical conformations of **3**−**5** rapidly interconvert in solution. Cyclic voltammograms of **3**−**5** show more reversible oxidations than model compounds lacking bridging sp^3 chains. These are the only double-helical molecules that do not feature bonding interactions between the helix strands, or covalent bonds to templates dispersed throughout the strands, or any type of encoding. The driving force for helix formation is analyzed.

Introduction

Of the many types of helical molecules,[1,2] double helices have captured the greatest attention.[2−8] The structure elucidation of the first compound recognized as a double helix, DNA,[3] has been immortalized in books and plays. Since this structural motif intrinsically shields interior functional domains, it represents an astute evolutionary choice for carrying the genetic code. However, we are not aware of any efforts to employ double helices as "protecting groups" for abiological functional arrays.

To our knowledge, all double-helical molecules feature either (1) bonding interactions between the helix strands, such as hydrogen bonds, or (2) covalent bonds to metal templates dispersed throughout the strands. Factors that promote or enforce complementarity, e.g., the programming[9] or "encoding of specific structural and conformational information",[4b] are thought to be required. We wondered whether it would be possible to design double-helical molecules that lack these conventional driving forces. In the extreme, might certain substances appear to yield double helices because "they felt like it"?

Toward this end, we sought rodlike building blocks, represented by **A** in Scheme 1. Such moieties are seeing extensive use in the development of molecular-scale devices.[10] The most

[†] Universität Erlangen-Nürnberg.
[‡] University of Utah.

(1) Meurer, K. P.; Vögtle, F. *Top. Curr. Chem.* **1985**, *127*, 1.
(2) (a) Piguet, C.; Bernardinelli, G.; Hopfgartner, G. *Chem. Rev.* **1997**, *97*, 2005. (b) Albrecht, M. *Chem. Rev.* **2001**, *101*, 3457. (c) Albrecht, M. *Angew. Chem., Int. Ed.* **2005**, *44*, 6448; *Angew. Chem.* **2005**, *117*, 6606.
(3) Watson, J. D.; Crick, F. H. C. *Nature* **1953**, *171*, 737 and 964.
(4) (a) Lehn, J.-M.; Rigault, A.; Siegel, J.; Harrowfield, J.; Chevrier, B.; Moras, D. *Proc. Natl. Acad. Sci. U.S.A.* **1987**, *84*, 2565. (b) Ohkita, M.; Lehn, J.-M.; Baum, G.; Fenske, D. *Chem.—Eur. J.* **1999**, *5*, 3471. (c) Funeriu, D. P.; Lehn, J.-M.; Fromm, K. M.; Fenske, D. *Chem.—Eur. J.* **2000**, *6*, 2103. (d) Berl, V.; Huc, I.; Khoury, R. G.; Lehn, J.-M. *Chem.—Eur. J.* **2001**, *7*, 2810.
(5) Mamula, O.; von Zelewsky, A.; Bark, T.; Bernardinelli, G. *Angew. Chem., Int. Ed.* **1999**, *38*, 2945; *Angew. Chem.* **1999**, *111*, 3129.
(6) Casnati, A.; Liantonio, R.; Metrangolo, P.; Resnati, G.; Ungaro, R.; Ugozzoli, F. *Angew. Chem., Int. Ed.* **2006**, *45*, 1915; *Angew. Chem.* **2006**, *118*, 1949.
(7) Goto, H.; Katagiri, H.; Furusho, Y.; Yashima, E. *J. Am. Chem. Soc.* **2006**, *128*, 7176.
(8) For other types of double helices based upon platinum phosphine or alkynyl complexes, see: (a) Peng, H.-Y.; Lam, C.-K.; Mak, T. C. W.; Cai, Z.; Ma, W.-T.; Li, Y.-X.; Wong, H. N. C. *J. Am. Chem. Soc.* **2005**, *127*, 9603. (b) Furusho, Y.; Tanaka, Y.; Yashima, E. *Org. Lett.* **2006**, *8*, 2583.
(9) Rowan, A. E.; Nolte, R. J. M. *Angew. Chem., Int. Ed.* **1998**, *37*, 63; *Angew. Chem.* **1998**, *110*, 65.
(10) (a) Schwab, P. F. H.; Levin, M. D.; Michl, J. *Chem. Rev.* **1999**, *99*, 1863. (b) Schwab, P. F. H.; Smith, J. R.; Michl, J. *Chem. Rev.* **2005**, *105*, 1197.

 10.1021/ja0716103 CCC: $37.00

Scheme 1. Design of Possible Double-Helical Molecules (**C**) and Some Alternative Conformations (**D**, **E**)

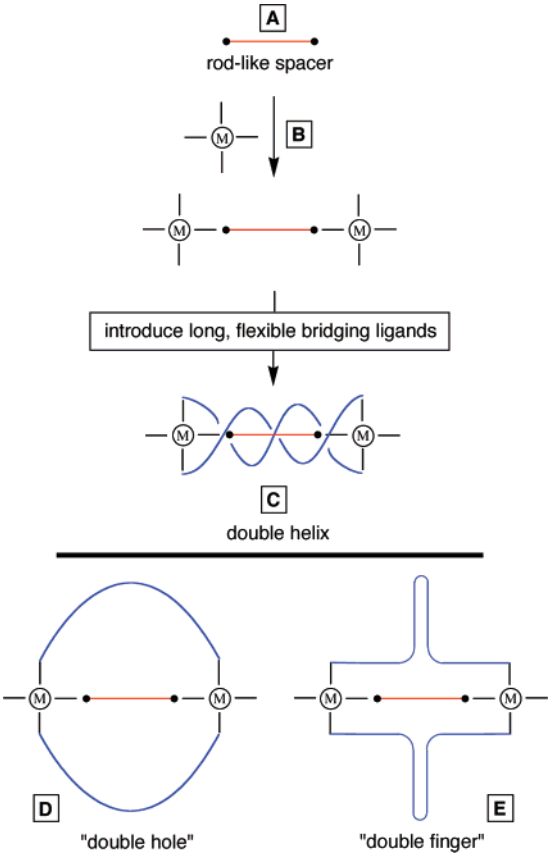

fundamental and radially compact would be a chain of sp hybridized carbons.[11] An atom that supports at least two additional bonds would then be grafted onto each terminus. Transition metals are obvious candidates,[12] as exemplified by the square planar endgroups **B** in Scheme 1. These could anchor two long flexible chains, containing for example polymethylene ($(CH_2)_m$) or polydifluoromethylene ($(CF_2)_m$) domains.

Conformation is then an issue. Will the flexible chains twist about the rod to give double helices as in the case of **C** (Scheme 1)? Alternatively, will they preferentially adopt conformations with "holes" (**D**) or "fingers" (**E**)? Since monocyclic crown ethers and related macrocycles seldom exhibit conformations with holes,[13] we discounted possibility **D**. However, **E** was viewed as a plausible alternative. Regardless, all of these conformations sterically shield the rodlike segment to varying degrees.

Such assemblies would have potential applications. For example, platinum(II)-capped polyynes $Pt(C{\equiv}C)_nPt$ (polyynediyls) with as many as 28 sp carbon atoms have been isolated,[14] corresponding to a metal−metal separation of 3.9 nm. However, all polyynes become increasingly more labile with sp carbon chain length. Since the decomposition pathways are believed to be bimolecular, systems of the type **C**−**E** should exhibit enhanced kinetic stabilities. New length regimes would likely be accessible.

Also, molecules in which unsaturated ligands span two transition metals can often be generated in more than one oxidation state, each of which can undergo interesting charge-transfer phenomena.[15] However, the stabilities of oxidized or reduced species derived from metal-capped polyynes dramatically decrease with sp chain length.[16] No examples with more than eight carbon atoms have been isolated,[17] hampering certain applications of these wirelike species. The flexible chains in **C**−**E** should again serve a stabilizing function, which for odd-electron systems would be conceptually analogous to the insulation about household electrical wire. Others have reported complementary approaches to shielding unsaturated assemblies that connect two electroactive groups.[18−21]

Hence, we set out to investigate whether $Pt(C{\equiv}C)_nPt$ moieties could serve as core units for double-helical assemblies **C**. One of several underlying considerations involved the well-established redox chemistry of monoplatinum(II) complexes. In most but not all cases, electrochemical oxidations to platinum(III) are only partially reversible.[22] Thus, it would be simple to qualitatively detect a stabilizing effect of the flexible chains upon the corresponding radical cations.

As summarized in Scheme 2, two synthetic strategies were considered. The first involved reactions of preformed $Pt(C{\equiv}C)_nPt$ species (**F**) with bis(α,ω-diarylphosphino)alkanes, in which the phosphorus atoms are separated by flexible polymethylene chains. This can be viewed as a coordination-driven "self-assembly" process with potential for operationally simple nanodevice synthesis. In terms of precedent, Sünkel had shown that when the chloride-substituted diplatinum ethynediyl complex $Cl(Ph_3P)_2PtC{\equiv}CPt(PPh_3)_2Cl$ was treated with excess PEt_3, all of the PPh_3 ligands could be replaced.[23]

The second strategy involved the synthesis of platinum chloride complexes with ω-functionalized *n*-alkyl *mono*phosphine ligands (**G**). The sp carbon chain would then be introduced, and the phosphine ligands on opposite platinum termini coupled, generating bridging diphosphines within the metal coordination sphere. In both approaches, there would be the possibility of byproducts in which the diphosphine ligands span *trans* positions of the same platinum atom, as shown in **H′**.

In this paper, we report successful syntheses of the target molecules **C** by the first strategy. This simple route allows rapid access to a number of complexes but also has limitations as described below. In the following paper, we report successful

(11) Szafert, S.; Gladysz, J. A. *Chem. Rev.* **2003**, *103*, 4175; **2006**, *106*, PR1-PR33.
(12) For a review of complexes of the formula $L_mMC_xML_m$, and related species, see: Bruce, M. I.; Low, P. J. *Adv. Organomet. Chem.* **2004**, *50*, 179.
(13) Gokel, G. W. *Crown Ethers and Cryptands*; Royal Society of Chemistry: Cambridge, U.K., 1991; Chapter 4.
(14) (a) Mohr, W.; Stahl, J.; Hampel, F.; Gladysz, J. A. *Chem.—Eur. J.* **2003**, *9*, 3324. (b) Zheng, Q.; Bohling, J. C.; Peters, T. B.; Frisch, A. C.; Hampel, F.; Gladysz, J. A. *Chem.—Eur. J.* **2006**, *12*, 6486.
(15) Paul, F.; Lapinte, C. In *Unusual Structures and Physical Properties in Organometallic Chemistry*; Gielen, M., Willem, R., Wrackmeyer, B., Eds.; Wiley: New York, 2002; pp 220−291.
(16) (a) Dembinski, R.; Bartik, T.; Bartik, B.; Jaeger, M.; Gladysz, J. A. *J. Am. Chem. Soc.* **2000**, *122*, 810. (b) Meyer, W. E.; Amoroso, A. J.; Horn, C. R.; Jaeger, M.; Gladysz, J. A. *Organometallics* **2001**, *20*, 1115.
(17) Coat, F.; Lapinte, C. *Organometallics* **1996**, *15*, 477.
(18) See: Frampton, M. J.; Anderson, H. L. *Angew. Chem., Int. Ed.* **2007**, *46*, 1028; *Angew. Chem.* **2007**, *119*, 1046; and earlier work of this group reviewed therein.
(19) Schenning, A. P. H. J.; Arndt, J.-D.; Ito, M.; Stoddart, A.; Schreiber, M.; Siemsen, P.; Martin, R. E.; Boudon, C.; Gisselbrecht, J.-P.; Gross, M.; Gramlich, V.; Diederich, F. *Helv. Chim. Acta* **2001**, *84*, 296.
(20) (a) Lee, D.; Swager, T. M. *Synlett* **2004**, 149. (b) Kwan, P. H.; Swager, T. M. *Chem. Commun.* **2005**, 5211.
(21) Li, C.; Numata, M.; Bae, A.-H.; Sakurai, K.; Shinkai, S. *J. Am. Chem. Soc.* **2005**, *127*, 4548.
(22) (a) Klein, A.; Kaim, W. *Organometallics* **1995**, *14*, 1176. (b) Klein, A.; Hasenzahl, S.; Kaim, W.; Fiedler, J. *Organometallics* **1998**, *17*, 3532.
(23) Sünkel, K.; Birk, U.; Robl, C. *Organometallics* **1994**, *13*, 1679.

Scheme 2. Synthetic Planning: Routes to Target Complexes

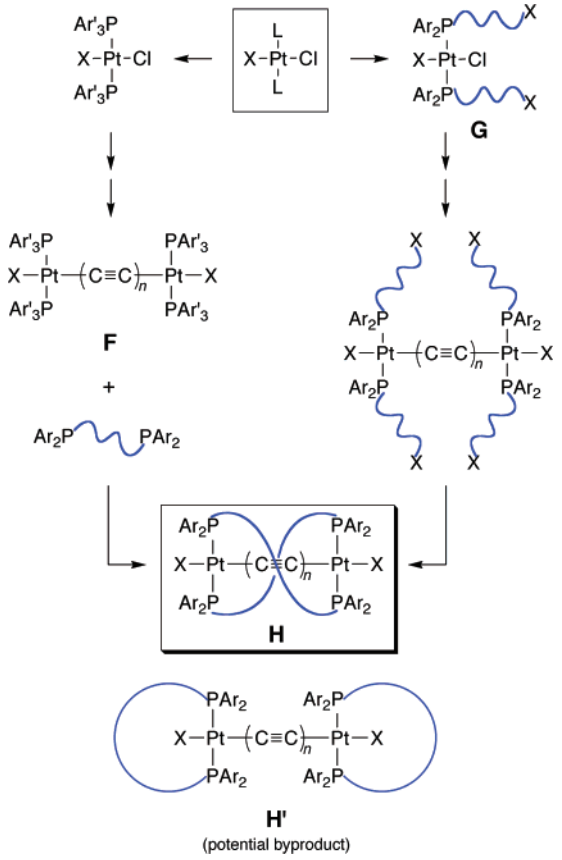

applications of the second strategy, using alkene metathesis as the means of ligand coupling.[24] This longer method is more reliable, but the overall yields are somewhat lower. Portions of this work have been communicated,[25] and additional details are described elsewhere.[26]

Results

1. Syntheses of Target Molecules: 8 sp and 14 sp^3 Carbons. Reactions of the *p*-tolyl-substituted diplatinum octatetraynediyl complex *trans*,*trans*-(*p*-tol)(Ph$_3$P)$_2$Pt(C≡C)$_4$Pt(PPh$_3$)$_2$(*p*-tol) (**1**; Scheme 3)[14b] were investigated first. An NMR tube was charged with **1** and the diphosphine Ph$_2$P(CH$_2$)$_{12}$PPh$_2$,[27,28] which features 12 sp^3 carbon atoms. Displacement of the PPh$_3$ ligands proceeded rapidly below room temperature, generating one platinum-containing product as assayed by ^{31}P NMR and TLC. However, when solutions were concentrated, insoluble, presumably oligomeric or polymeric materials formed. Only small portions could be induced to redissolve.

Comparable results were obtained with the longer-chain diphosphine Ph$_2$P(CH$_2$)$_{16}$PPh$_2$.[28] Extensive attempts to crystallize the major products from dilute solutions were unsuccessful. Oligomeric structures are rigorously established for similar Pt-

Scheme 3. First Attempt to Synthesize Target Complexes

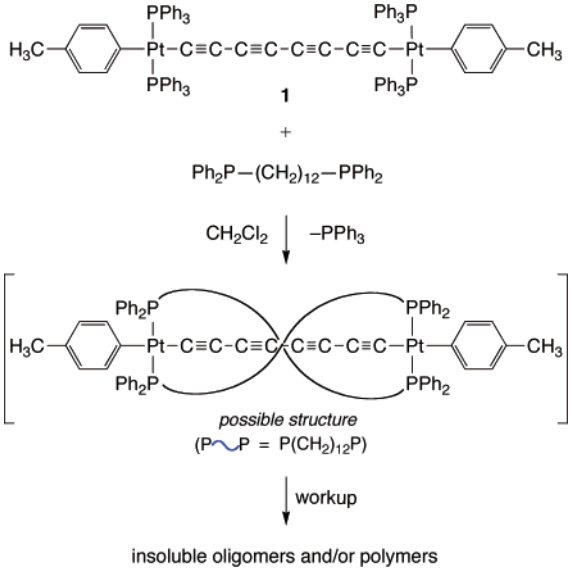

(C≡C)$_n$Pt-derived materials below. Monoplatinum complexes of other types of long-chain chelating diphosphines have also been observed to oligomerize.[28b]

In an attempt to avoid the generation of oligomers, two strategy modifications were implemented: (a) platinum endgroups with enhanced Lewis acidities were targeted, with the idea that the dissociation of one terminus of the diphosphine ligand in **H** (Scheme 2) would be retarded − a logical initial event in oligomerization; (b) since this might in turn render substitution reactions of **F** (Scheme 2) more difficult, approaches involving functionalized phosphines (**G**) were investigated. In this way, no platinum−phosphorus bond-making or -breaking reactions are required after the initial substitution. As described in the following paper,[24] this sequence proved successful with pentafluorophenyl-substituted platinum endgroups and provided the first syntheses of the target molecules. However, an obvious question remained: would modification (a) alone have sufficed?

As shown in Scheme 4, the answer is in many cases yes. A CH$_2$Cl$_2$ solution of the diphosphine Ph$_2$P(CH$_2$)$_{14}$PPh$_2$ (2.6 equiv),[27] which features 14 sp^3 carbon atoms, was added to a moderately dilute CH$_2$Cl$_2$ solution of the pentafluorophenyl-substituted diplatinum complex *trans*,*trans*-(C$_6$F$_5$)(*p*-tol$_3$P)$_2$Pt(C≡C)$_4$Pt(P*p*-tol$_3$)$_2$(C$_6$F$_5$) (**2**; 0.0025 M).[14a] Workup gave the target complex *trans*,*trans*-(C$_6$F$_5$)(Ph$_2$P(CH$_2$)$_{14}$PPh$_2$)Pt(C≡C)$_4$Pt(Ph$_2$P(CH$_2$)$_{14}$PPh$_2$)(C$_6$F$_5$) (**3**) as an analytically pure yellow powder in 87% yield. The structure was verified crystallographically, as described below. Analogous reactions with similar phenyl-substituted diphosphines, (*p*-RC$_6$H$_4$)$_2$P(CH$_2$)$_{14}$P(*p*-C$_6$H$_4$R)$_2$ (R = CH$_3$, *t*-Bu),[30] gave the corresponding complexes **4** and **5** in 77−91% yields.

Complexes **3**−**5**, and all other compounds isolated below, were stable in air as solids for extended periods. They were characterized by IR, NMR (^{1}H, ^{13}C, ^{31}P), and UV−visible

(24) de Quadras, L.; Bauer, E. B.; Mohr, W.; Bohling, J. C.; Peters, T. B.; Martín-Alvarez, J.; Hampel, F.; Gladysz, J. A. *J. Am. Chem. Soc.* **2007**, *129*, 8296.
(25) (a) Stahl, J.; Bohling, J. C.; Bauer, E. B.; Peters, T. B.; Mohr, W.; Martín-Alvarez, J. M.; Hampel, F.; Gladysz, J. A. *Angew. Chem., Int. Ed.* **2002**, *41*, 1871; *Angew. Chem.* **2002**, *114*, 1951. (b) See also: Owen, G. R.; Stahl, J.; Hampel, F.; Gladysz, J. A. *Organometallics* **2004**, *23*, 5889.
(26) (a) Mohr, W. Doctoral Dissertation, Universität Erlangen-Nürnberg, 2002. (b) Stahl, J. Doctoral Dissertation, Universität Erlangen-Nürnberg, 2003.
(27) Mohr, W.; Horn, C. R.; Stahl, J.; Gladysz, J. A. *Synthesis* **2003**, 1279.
(28) (a) Hill, W. E.; McAuliffe, C. A.; Niven, I. E.; Parish, R. V. *Inorg. Chim. Acta* **1980**, *38*, 273. (b) Hill, W. E.; Minahan, D. M. A.; Taylor, J. G.; McAuliffe, C. A. *J. Am. Chem. Soc.* **1982**, *104*, 6001.
(29) A similar reaction of the Pt(C≡C)$_8$Pt homologue[14a] of **2** and **10** with Ph$_2$P(CH$_2$)$_{28}$PPh$_2$ gave exclusively oligomeric products.
(30) de Quadras, L.; Stahl, J.; Zhuravlev, F.; Gladysz, J. A. *J. Organomet. Chem.* **2007**, *692*, 1859.

spectroscopy, and mass spectrometry, as summarized in the Experimental Section. The IR and UV−visible spectra were quite similar to those of the precursor **2**[14a] and essentially identical with those of the model compound **6**.[30] The latter is a

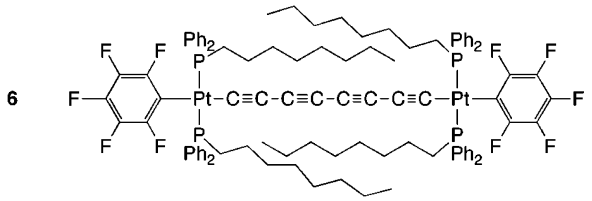

better electronic model for **3**, lacking only bridging sp³ carbon chains. The Pt*C*≡*C* ^{13}C NMR signals of **3**−**5** (98.6/94.2, 99.2/94.1, 99.1/94.4 ppm) differed slightly from those of **2** (100.6/96.7) but were nearly identical with those of **6** (100.0/94.2 ppm). The P*C*H$_2$*C*H$_2$*C*H$_2$ ^{13}C NMR signals were also very close to those of **6** (28.1−28.3/25.5−25.7/30.6−30.7 vs 28.2/25.5/31.3 ppm). The mass spectra exhibited intense molecular ions (100%). DSC data for **3** and **4** showed endotherms at 244 and 213 °C (T_e; presumably phase transitions) with exotherms beginning at higher temperatures (271 and 260 °C, T_i) that were accompanied by mass loss (TGA data).

2. Crystallography: 8 sp and 14 sp³ Carbons. Complexes **3**, **4**, and **5** readily crystallized. The first was obtained as both benzene and toluene sesquisolvates (**3**·(benzene)$_{1.5}$, **3**·(toluene)$_{1.5}$), and the last, as two different toluene solvates (**5**·(toluene)$_{5.5}$ and **5**·(toluene)$_2$) or pseudopolymorphs.[33] The crystal structures were solved as summarized in the Supporting Information. Those of **3**·(benzene)$_{1.5}$ and **3**·(toluene)$_{1.5}$ were very similar. Key metrical parameters are given in Tables 1−3.

The structures of **3**·(toluene)$_{1.5}$, **4**, and **5**·(toluene)$_{5.5}$ are compared in Figure 1 (**I**−**K**). In all three compounds, the sp³ carbon chains exhibit a striking double-helical conformation. Helices are intrinsically chiral, and both enantiomers are present in the crystal lattice. With **3**·(benzene)$_{1.5}$ and **3**·(toluene)$_{1.5}$, the twisting is less "uniform" than that in the other complexes, a feature that can be analyzed via torsion angle patterns (Table 3) as described below. The idealized structures (i.e., as represented in Scheme 4) belong to the point group D_2.

The bond lengths, bond angles, and slight sp chain curvatures in **3**·(toluene)$_{1.5}$, **4**, and **5**·(toluene)$_{5.5}$ are unexceptional. They are very close to those of **2**,[14a] which lacks bridging diphosphines, as well as higher and lower homologues.[14a,25b] Considerably greater sp chain curvature has been observed,[11] a normal phenomenon that has various measures, such as the average bond angles in Table 1 or the difference between the platinum−platinum distances and the sum of the intervening bond lengths. These parameters and others have been analyzed for all Pt(C≡C)$_n$Pt complexes in detail elsewhere.[11]

The angles defined by the square planes of the platinum termini are of particular interest. Of the measures summarized in Table 1, we favor the planes defined by the P−Pt−P linkage on one endgroup and the platinum on the other. These emphasize the twist defined by the P−Pt−P linkages and are less effected by various geometric nonidealities. The values in **3**·(benzene)$_{1.5}$,

Scheme 4. Reactions of the Pt(C≡C)$_4$Pt Complex **2** with Bis(α,ω-diarylphosphino)alkanes

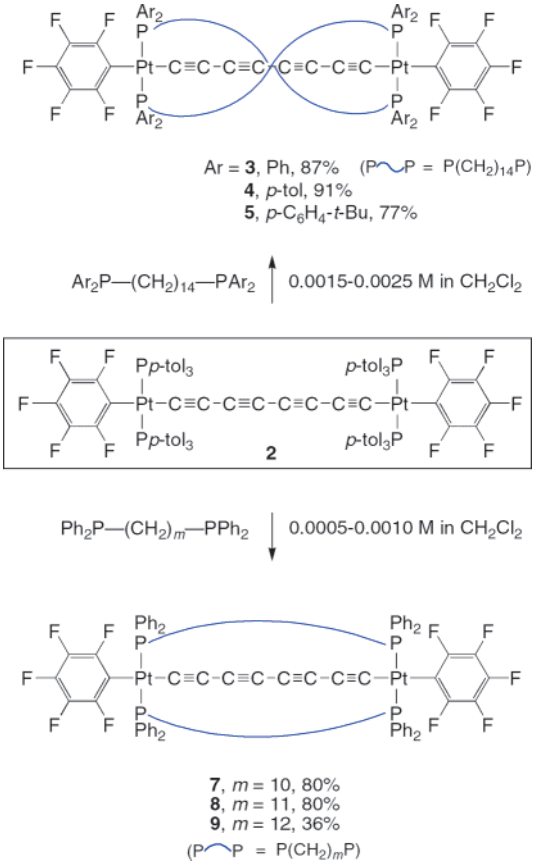

3·(toluene)$_{1.5}$, **4**, and **5**·(toluene)$_{5.5}$ range from 189.8° to 196.6°, more than a half twist. This feature is emphasized in the partial structure of **3**·(toluene)$_{1.5}$ shown in Figure 2 (**L**). Helical objects are also characterized by a degree of helicity and a pitch (Table 1).[1,31] The former is derived by dividing the preceding angles by 360°, and the latter represents the hypothetical distance at which a full turn would be reached.

The crystal structure of precursor **2** has been previously reported,[14a] and two views with all atoms at van der Waals radii are illustrated in Figure 3 (**M**, **N**; parallel and perpendicular to the planes of the C_6F_5 rings). The sp carbon chain is clearly accessible to external reagents. Figure 3 also gives analogous representations of **3**·(toluene)$_{1.5}$ (**Q**, **R**), as well as structures from which the phenyl rings and hydrogen atoms are omitted (**O**, **P**). For reference, comparable views of **4** are depicted (**S**, **T**); **5**·(toluene)$_{5.5}$ is very similar. These structures nicely illustrate the extensive shielding of the sp chains in **3**−**5**, although **R** and **T** reveal that a line-of-sight through a protecting rim of peripheral groups remains.

Figure 3 shows that the sp and sp³ carbon chains of **3**·(toluene)$_{1.5}$ and **4** entwine with a spacing slightly greater than their van der Waals radii (1.78 and 1.70 Å).[32] A cylindrical helix is characterized by a radius, which can be approximated by calculating the average distances of the sp³ carbon atoms from the platinum−platinum vectors. As summarized in Table 1, these span the narrow range from 3.977 to 4.053 Å. A higher value indicates a "looser" helix. Accordingly, there is an inverse correlation with the degree of helicity. The packing diagrams show essentially parallel sp chains, the spacing between which

(31) Gray, A. The Helix and its Generalizations. In *Modern Differential Geometry of Curves and Surfaces with Mathematica*, 2nd ed.; CRC Press: Boca Raton, FL, 1997; pp 198−200.
(32) Bondi, A. *J. Phys. Chem.* **1964**, *68*, 441.
(33) Threlfall, T. L. *Analyst* **1995**, *120*, 2435.

Table 1. Key Crystallographic Distances [Å] and Angles [deg] for Helical Complexes

complex	**3**·(benzene)$_{1.5}$[a]	**3**·(toluene)$_{1.5}$	**4**	**5**·(toluene)$_{5.5}$	**11**·(CH$_2$Cl$_2$)$_{0.67}$[b]
Pt•••Pt	12.775(8)	12.7653(14)	12.6984(5)	12.8867(3)	17.9897(8)
sum of bond lengths, Pt1 to Pt2	12.956	12.914	12.890	12.896	18.023
Pt1−C1	2.003(3)	1.987(4)	1.991(8)	1.988(4)	1.962(13)
C1−C2	1.207(5)	1.215(7)	1.211(9)	1.205(6)	1.207(19)
C2−C3	1.368(5)	1.365(7)	1.345(10)	1.369(6)	1.38(2)
C3−C4	1.207(5)	1.214(7)	1.201(9)	1.206(6)	1.23(2)
C4−C5	1.354(5)	1.360(7)	1.363(10)	1.360(6)	1.37(2)
C5−C6	1.216(5)	1.207(7)	1.198(9)	1.209(6)	1.16(2)
C6−C7	1.368(5)	1.360(7)	1.372(10)	1.356(6)	1.36(2)
C7−C8	1.209(5)	1.212(6)	1.222(9)	1.220(6)	1.22(2)
C8−C9	-	-	-	-	1.34(2)
C9−C10	-	-	-	-	1.21(2)
C10−C11	-	-	-	-	1.41(2)
C11−C12	-	-	-	-	1.176(19)
C8−Pt2 or C12−Pt2	1.994(3)	1.994(4)	1.987(7)	1.983(4)	1.998(15)
Pt1−C1−C2	178.0(3)	175.9(5)	178.8(6)	179.3(4)	179.0(14)
C1−C2−C3	177.5(4)	178.9(6)	176.4(8)	178.3(5)	174.7(18)
C2−C3−C4	177.3(4)	178.4(6)	176.0(8)	179.9(7)	178(2)
C3−C4−C5	176.9(5)	178.2(6)	175.3(8)	178.5(6)	177(2)
C4−C5−C6	178.5(5)	177.0(6)	176.0(8)	177.9(6)	174(2)
C5−C6−C7	176.3(4)	177.3(6)	177.9(8)	178.5(5)	174(2)
C6−C7−C8	174.1(4)	172.8(5)	178.2(8)	179.1(5)	178(2)
C7−C8−C9	-	-	-	-	177(3)
C8−C9−C10	-	-	-	-	180(3)
C9−C10−C11	-	-	-	-	176.9(18)
C7−C8−Pt2 or C11−C12−Pt2	171.7(3)	171.6(4)	171.5(6)	179.3(4)	177.8(15)
av Pt−C_{sp}−C_{sp}	174.9	173.8	175.2	179.3	178.4
av C_{sp}−C_{sp}−C_{sp}	176.8	177.1	176.6	178.7	176.6
av sp/sp^3 distance[c]	4.053	3.977	4.042	3.988	3.868
av π stacking[d]	3.896	3.755	3.772	3.704	3.907
P−Pt−P/Pt angle[e]	196.6	196.5	189.9	193.3	163.2
Pt+P+P+C_i+C1 angle[e]	198.1	200.8	188.6	193.5	163.9
helix pitch[f]	23.72	23.66	24.45	24.02	39.76
degree of helicity	54.6%	54.6%	52.7%	53.7%	45.3%
C_{sp}−C_{sp}[g]	8.071	7.974	9.339	11.959	9.028
fractional offset[h]	0.55	0.38	0.49	0.44	0.44

[a] In order to better compare the two similar noncentrosymmetric solvates of **3**, the numbering of the PtC$_8$Pt segment in **3**·(benzene)$_{1.5}$ has been reversed in this table. [b] Data for the nonhelical molecule in the unit cell is given in Table 2. [c] Average distance from every CH_2 group to the Pt−Pt vector. [d] Distance between midpoints of the C_6F_5 and C_6H_4R rings. [e] Angle between planes defined by these atoms on each endgroup. [f] The hypothetical distance at which a full helix turn is reached. [g] The shortest carbon−carbon distance between parallel sp chains in the crystal lattice. [h] Of parallel sp chains: see ref 11.

increases from 7.97 to 11.96 Å as the sizes of the *p*-aryl substituents increases (Table 1).

In contrast to the preceding four crystal structures, that of the pseudopolymorph **5**·(toluene)$_2$ exhibited a nonhelical conformation. As shown in Figure 4, the sp^3 carbon chains define loops with respect to the sp chain. However, when atoms are viewed at van der Waals radii, there are no "holes" as in the case of **D** (Scheme 1). The average distance of the sp^3 carbon atoms from the platinum−platinum vector (Table 2) is somewhat greater than that in helical **5**·(toluene)$_{5.5}$ (4.064 vs 3.988 Å). Interestingly, the crystal density of **5**·(toluene)$_2$, a property sometimes used to gauge the relative stabilities of polymorphs,[33] is higher than that of **5**·(toluene)$_{5.5}$ (1.333 vs 1.256 Mg/m^3); in contrast to the other structures, the lattice features *two* nonparallel sets of parallel sp chains. In any event, **V** and **W** (Figure 4) show that the sp chain in **5**·(toluene)$_2$ is only slightly less shielded than those in the helical complexes. Importantly, the structure requires that nonhelical conformations of **5** be populated in solution.

In all of the preceding structures, including that of **2**, aryl/C_6F_5/aryl stacking interactions are evident. These are found for nearly all (C_6F_5)Pt adducts of aryl phosphines,[14a,25b,34,35] and average distances are summarized in Tables 1 and 2. The origin of this phenomenon, which is general for highly fluorinated arenes, is well understood.[36] Although it plays a role in crystal packing, it is not believed to be a determinant of sp^3 chain conformation in the title molecules. Note that the shortest average distance is found in nonhelical **5**·(toluene)$_2$.

3. Syntheses of Target Molecules: Other sp/sp^3 Carbon Chain Lengths. Several questions follow from the preceding results: (a) How short an sp^3 carbon chain can be introduced? (b) How long an sp^3 carbon chain can be introduced? (c) Can analogous chemistry be effected with longer sp carbon chains? When the sp^3/sp carbon ratio becomes too small, helical conformations should no longer be possible. However, such species would still possess sp carbon chains that are to various degrees sterically protected. Furthermore, when the sp^3 and sp chains have similar numbers of atoms, they are constrained over

(34) Bauer, E. B.; Hampel, F.; Gladysz, J. A. *Organometallics* **2003**, *22*, 5567.
(35) Shima, T.; Bauer, E. B.; Hampel, F.; Gladysz, J. A. *Dalton Trans.* **2004**, 1012.
(36) Reichenbächer, K.; Süss, H. I.; Hullinger, J. *Chem. Soc. Rev.* **2005**, *34*, 20.

Table 2. Key Crystallographic Distances [Å] and Angles [deg] for Nonhelical Complexes

complex	**5**·(toluene)$_2$[a]	**7**·(toluene)$_4$	**7**·(CHCl$_3$)$_2$	**9**·(CH$_2$Cl$_2$)$_{2.5}$	**11**·(CH$_2$Cl$_2$)$_{0.67}$[a,b]
Pt•••Pt	12.8820(21)	12.9120(3)	12.6417(31)	12.9580(2)	17.6087(13)
sum of bond lengths, Pt1 to Pt2	12.907	12.933	12.953	12.980	18.06
Pt1−C1	1.989(7)	2.014(6)	1.998(5)	2.009(4)	1.960(16)
C1−C2	1.220(9)	1.192(8)	1.219(6)	1.205(6)	1.23(2)
C2−C3	1.356(10)	1.366(8)	1.359(7)	1.379(6)	1.36(2)
C3−C4	1.202(10)	1.208(8)	1.224(7)	1.214(7)	1.19(2)
C4−C5	1.377(15)	1.361(9)	1.362(6)	1.365(7)	1.38(3)
C5−C6	-	1.215(8)	1.212(6)	1.222(7)	1.24(2)
C6−C7	-	1.368(8)	1.369(6)	1.365(6)	1.34(4)
C7−C8	-	1.210(8)	1.209(6)	1.212(6)	-
C8−Pt2	-	1.999(6)	2.001(4)	2.009(4)	-
Pt1−C1−C2	175.7(7)	174.0(6)	171.1(4)	176.0(5)	166.7(14)
C1−C2−C3	175.6(8)	178.2(8)	176.4(6)	178.5(6)	170.8(18)
C2−C3−C4	179.4(10)	178.3(7)	177.4(5)	178.9(6)	174.5(18)
C3−C4−C5	178.8(12)	178.5(9)	177.4(5)	179.6(6)	176(2)
C4−C5−C6	-	179.6(9)	177.0(5)	179.2(6)	178(2)
C5−C6−C7	-	178.5(8)	175.0(5)	178.6(5)	178(2)
C6−C7−C8	-	177.5(7)	173.5(5)	178.7(5)	-
C7−C8−Pt2	-	176.7(6)	169.4(4)	175.1(4)	-
av Pt−C_{sp}−C_{sp}	175.7	175.4	170.3	175.6	166.7
av C_{sp}−C_{sp}−C_{sp}	177.9	178.4	176.1	178.9	175.5
av sp/sp³ distance[c]	4.064	3.932	3.989	4.090	4.157
av π stacking[d]	3.633	3.803	3.756	3.766	3.979
P−Pt−P/Pt angle[e]	0.0	0.2	5.1	12.9	0.0
Pt+P+P+C_i+C1 angle[e]	0.0	2.7	40.4	18.3	0.0
C_{sp}−C_{sp}[f]	11.433	7.296	7.780	9.738	9.028
fractional offset[g]	0.88	0.41	0.10	0.32	-

[a] This molecule exhibits an inversion center. [b]Data for the helical molecule in the unit cell is given in Table 1. [c]Average distance from every CH_2 group to the Pt−Pt vector. [d]Distance between midpoints of the C_6F_5 and C_6H_4R rings. [e]Angle between planes defined by these atoms on each endgroup. [f]The shortest carbon−carbon distance between parallel sp chains in the crystal lattice. [g]Of parallel sp chains: see ref 11.

Table 3. Torsion Angles [deg] Involving sp³ Carbon Atoms for $Ar_2P(CH_2)_{14}PAr_2$-Bridged Complexes

complex	**3**·(benzene)$_{1.5}$[a]	**3**·(toluene)$_{1.5}$[a]	**4**[a]	**5**·(toluene)$_{5.5}$[a]	**5**·(toluene)$_2$
P−C1−C2−C3	−158.8/−80.8	−161.2/85.3	175.2/170.2	178.3/−179.4	177.9/−170.6
C1−C2−C3−C4	66.5/−71.9	64.6/−173.8	54.9/64.3	66.8/64.9	173.5/−68.8
C2−C3−C4−C5	171.4/173.3	173.2/166.5	62.1/62.1	63.9/64.4	69.2/−89.8[b]
C3−C4−C5−C6	−174.9/176.9	179.0/−176.4	174.8/179.5	169.9/174.9	176.8/−160.4[b]
C4−C5−C6−C7	−174.8/166.5	−176.3/170.1	−172.1/179.5	173.1/179.2	−179.3/−82.1[b]
C5−C6−C7−C8	175.8/−172.6	−178.6/173.1	175.2/−177.0	−178.5/−178.7	−160.9[b]/148.0[b]
C6−C7−C8−C9	66.6/173.6	67.8/61.9	172.3/178.2	170.2/170.7	−84.6[b]/−84.6[b]
C7−C8−C9−C10	173.4/171.1	171.5/172.1	−175.8/176.2	179.6/178.7	148.0[b]/−160.9[b]
C8−C9−C10−C11	173.8/68.5	174.1/172.4	176.2/−176.4	178.7/177.7	−82.1[b]/−179.3
C9−C10−C11−C12	173.2/166.0	174.2/177.9	−164.4/179.0	178.0/173.2	−160.4[b]/176.8
C10−C11−C12−C13	58.0/172.0	57.0/165.3	68.3/61.9	65.9/62.7	−89.8[b]/69.2
C11−C12−C13−C14	57.1/74.9	57.1/69.2	−176.1/55.3	63.3/63.4	−68.8/173.5
C12−C13−C14−P′	177.7/−158.6	−179.4/−150.9	169.4/171.6	−179.8/175.4	−170.6/177.9

[a] The sp³ carbon chains in these structures are not equivalent. The torsion angles for both are presented starting from the same platinum atom. [b]There is considerable vibrational disorder associated with the atoms from which these values are derived.

their entire lengths to be in close proximity, providing a valuable reference state.

As shown in Scheme 4 (bottom), CH_2Cl_2 solutions of the shorter-chain diphosphines $Ph_2P(CH_2)_mPPh_2$ (m = 10, 11, 12)[27,28] were added to CH_2Cl_2 solutions of **2** that were more dilute than those employed above. Workups gave the substitution products **7**, **8**, and **9** in 80%, 80%, and 36% yields, respectively. In the last reaction, which is closely related to the unsuccessful synthesis in Scheme 3, oligomeric byproducts were evident, and a higher dilution was necessary ([**2**] = 0.0005 M). The IR, NMR, UV−visible, MS, and DSC/TGA properties of **7**−**9** were very similar to those of **3**−**5**, including the ^{13}C NMR chemical shifts of the sp and sp³ carbon atoms.

Analogous reactions of longer-chain diphosphines $Ph_2P(CH_2)_mPPh_2$ (m = 16, 18, 32)[27,28] with highly dilute CH_2Cl_2 solutions of **2** (0.0001, 0.0001, 0.000 075 M) gave only insoluble oligomers (85%, 94%, 61%, respectively).[26a] The IR spectra of these materials were very similar. Mass spectra did not exhibit any ions for diplatinum complexes.

As shown in Scheme 5 (top), a CH_2Cl_2 solution of the diphosphine $Ph_2P(CH_2)_{18}PPh_2$ was added to an extremely dilute CH_2Cl_2 solution of the diplatinum dodecahexaynediyl or Pt-(C≡C)$_6$Pt complex **10** (0.000 03 M).[14a] Workup and crystallization gave the substitution product **11**, which has sp and sp³ chains of 12 and 18 carbon atoms, in 27% yield. Oligomeric material was also isolated in 64% yield. As with **3**−**9**, the IR

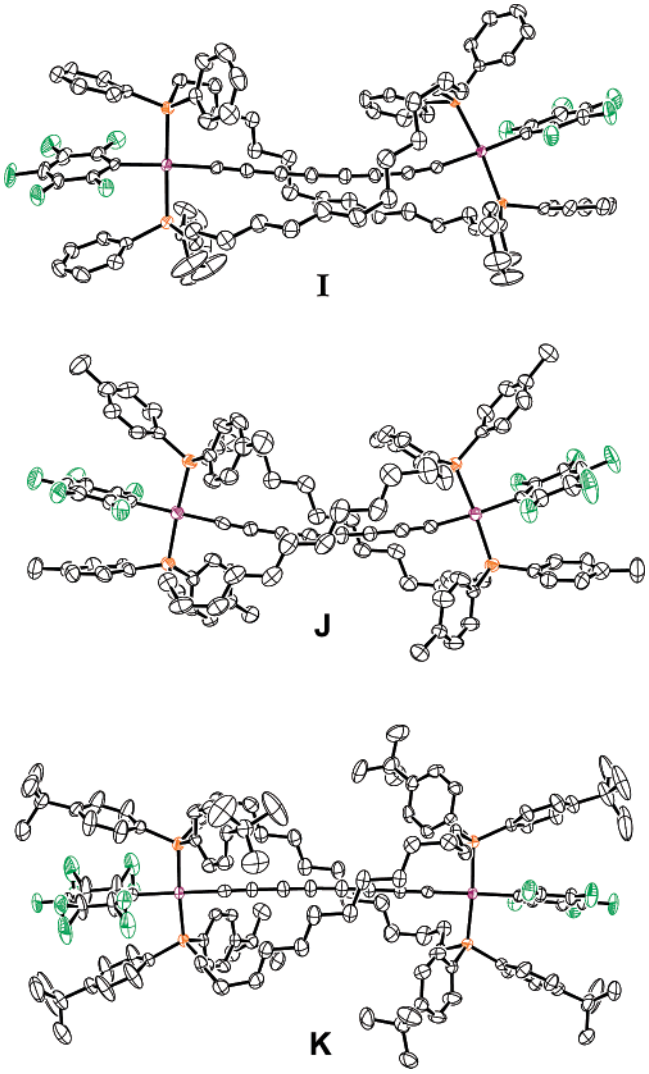

Figure 1. Thermal ellipsoid plots (50% probability level) of the double-helical $Pt(C{\equiv}C)_4Pt$ complexes with hydrogen atoms and solate molecules omitted: **I**, **3**·$(toluene)_{1.5}$; **J**, **4**; **K**, **5**·$(toluene)_{5.5}$.

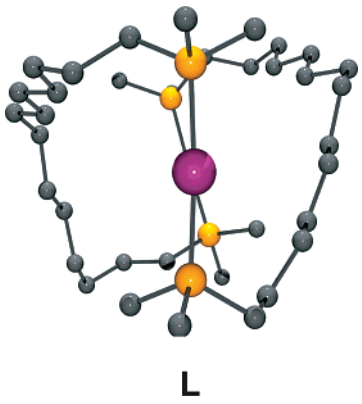

Figure 2. View of **3**·$(toluene)_{1.5}$ along the platinum−platinum axis with non-*ipso* aryl carbon atoms, hydrogen atoms, and solvate molecules omitted.

and UV−visible properties, and ^{13}C NMR chemical shifts of the sp carbon atoms, were similar to those of the unbridged precursor. However, as summarized in Scheme 5 (bottom), reactions of **10** and longer-chain diphosphines gave almost exclusively oligomeric products.[29] In the cases of $Ph_2P(CH_2)_{19}PPh_2$ and $Ph_2P(CH_2)_{20}PPh_2$, mass spectra of the reaction mixtures showed ions for diplatinum complexes, and trace amounts could be extracted from the oligomers.

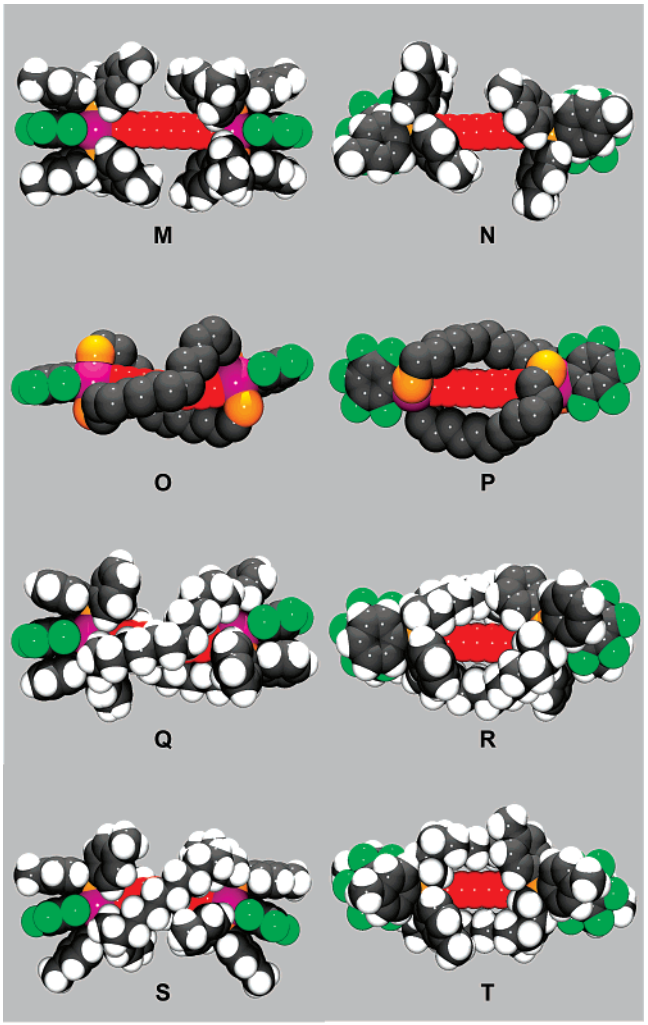

Figure 3. Space filling representations of selected $Pt(C{\equiv}C)_4Pt$ complexes: **M**, **N**, views of **2**·(toluene) parallel and perpendicular to the planes of the C_6F_5 ligands; **O**, **P**, analogous views of **3**·$(toluene)_{1.5}$ with phenyl rings, hydrogen atoms, and solvate molecules omitted; **Q**, **R**, analogous views of **3**·$(toluene)_{1.5}$ but with phenyl rings and hydrogen atoms; **S**, **T**, analogous views of **4**.

Experiments were conducted to confirm the oligomeric nature of these products. First, the material derived from **10** and $Ph_2P(CH_2)_{20}PPh_2$ gave an appropriate microanalysis. Second, it was treated with an excess of the monophosphine PEt_3. Trialkylphosphines are commonly more basic than diarylalkylphosphines. As shown in Scheme 5, substitution occurred to give the known complex *trans*,*trans*-$(C_6F_5)(Et_3P)_2Pt(C{\equiv}C)_6Pt(PEt_3)_2(C_6F_5)$ (**12**), which was isolated in 56% yield.[14a] Analogous additions of PEt_3 to oligomers derived from **2** and $Ph_2P(CH_2)_mPPh_2$ (m = 16, 18, 32) similarly gave *trans*,*trans*-$(C_6F_5)(Et_3P)_2Pt(C{\equiv}C)_4Pt(PEt_3)_2(C_6F_5)$.[14a]

4. Crystallography: Other sp/sp^3 Carbon Chain Lengths. Complexes **7**, **9**, and **11** could also be crystallized. In the case of **7**, two pseudopolymorphs, **7**·$(toluene)_4$ and **7**·$(CHCl_3)_2$, were obtained. Their crystal structures, and those of **9**·$(CH_2Cl_2)_{2.5}$ and **11**·$(CH_2Cl_2)_{0.67}$, were determined as summarized in the Supporting Information. Portions of the sp^3 carbon chains of **7**·$(toluene)_4$ and **9**·$(CH_2Cl_2)_{2.5}$ were disordered, but this could

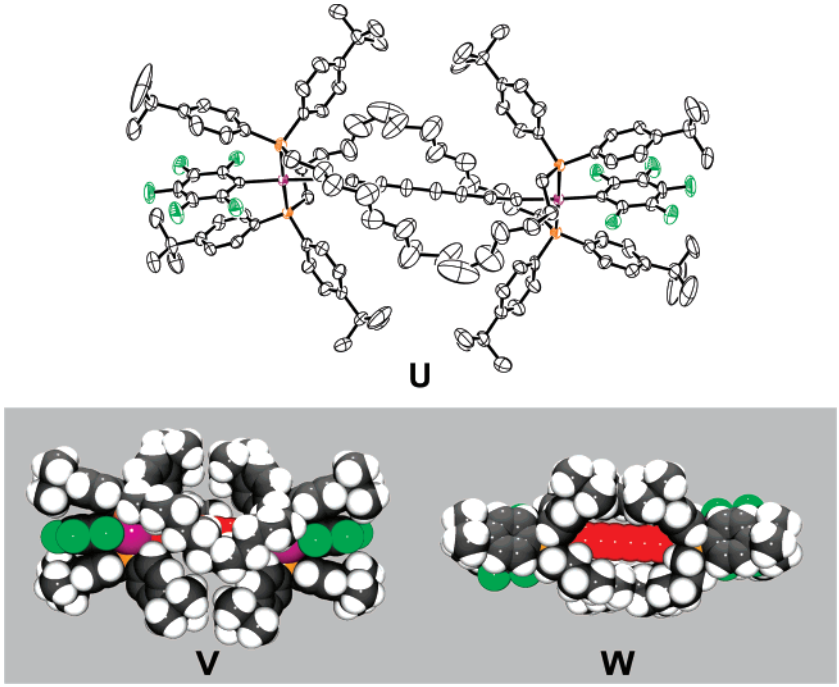

Figure 4. Structure of the nonhelical $Pt(C{\equiv}C)_4Pt$ complex **5**·(toluene)$_2$ with solvate molecules omitted: **U**, thermal ellipsoid plot (50% probability level) with hydrogen atoms omitted; **V**, **W**, views parallel and perpendicular to the planes of the C_6F_5 ligands with atoms at van der Waals radii.

Scheme 5. Reactions of the $Pt(C{\equiv}C)_6Pt$ Complex **10** with Bis(α,ω-diphenylphosphino)alkanes

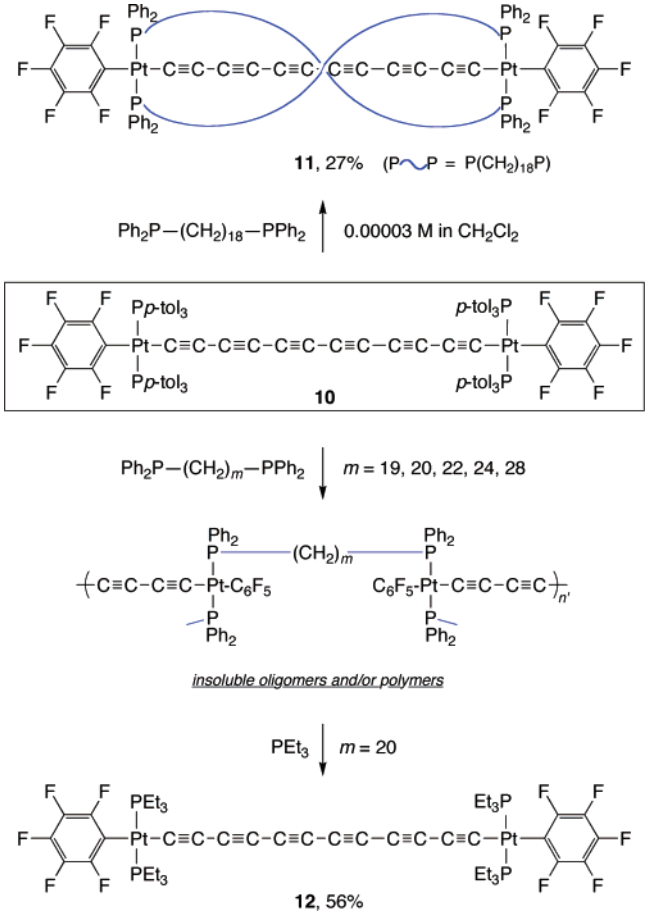

be resolved and only data for the dominant conformations are presented. Key metrical parameters are listed in Table 2. The structures of **7**·(toluene)$_4$, **7**·$(CHCl_3)_2$, and **9**·$(CH_2Cl_2)_{2.5}$ are shown in Figure 5. In all three cases, the angles defined by the P−Pt−P/Pt planes were near 0° (0.2°−12.9°).

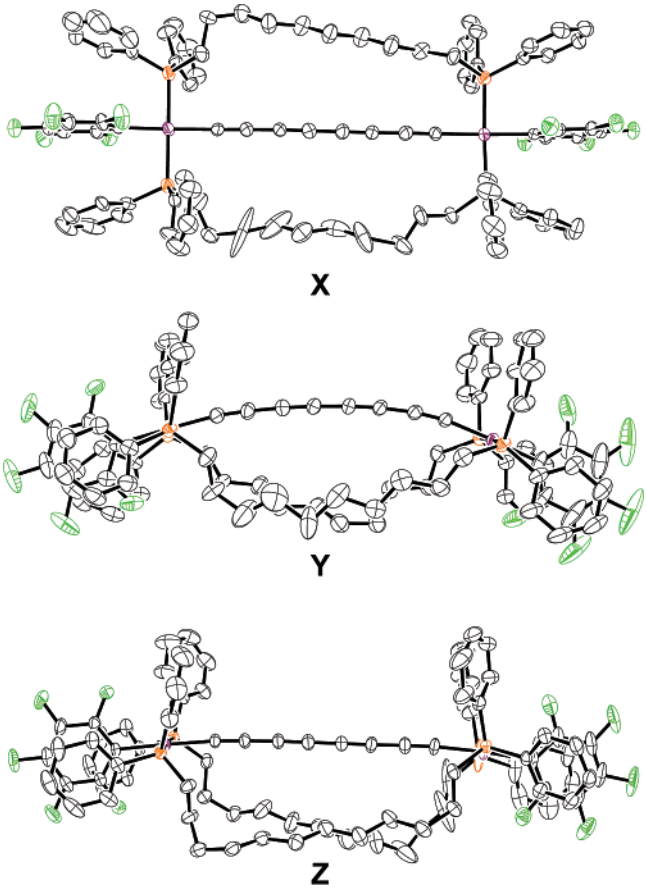

Figure 5. Thermal ellipsoid plots (50% probability level) of other nonhelical $Pt(C{\equiv}C)_4Pt$ complexes with hydrogen atoms and solvate molecules omitted: **X**, **7**·(toluene)$_4$ (dominant conformation); **Y**, **7**·$(CHCl_3)_2$; **Z**, **9**·$(CH_2Cl_2)_{2.5}$ (dominant conformation).

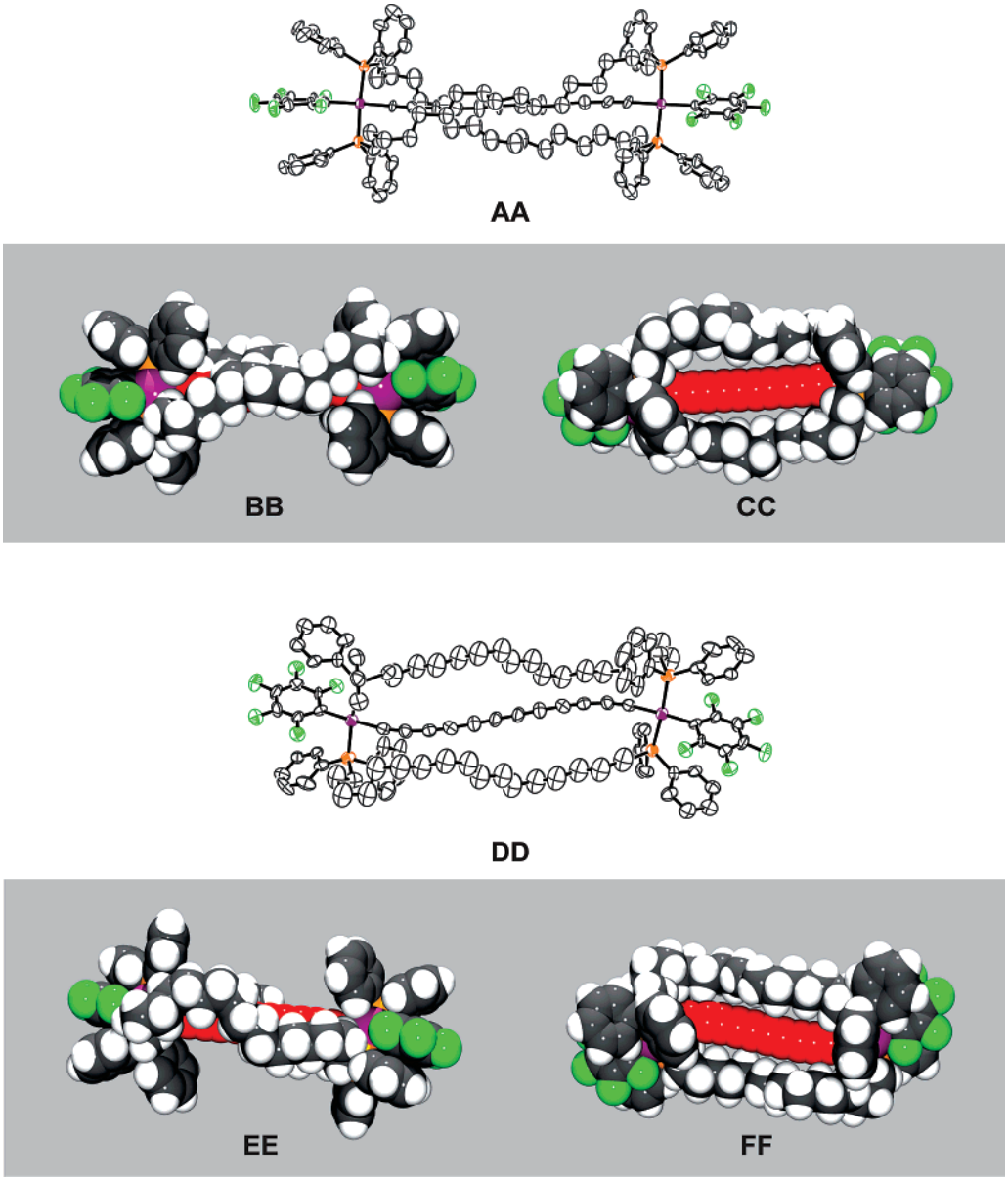

Figure 6. Structures of the two independent $Pt(C{\equiv}C)_{12}Pt$ complexes in crystalline **11**·$(CH_2Cl_2)_{0.67}$ with solvate molecules omitted: **AA**, thermal ellipsoid plot (50% probability level) of the double-helical complex with hydrogen atoms omitted; **BB**, **CC**, views parallel and perpendicular to the planes of the C_6F_5 ligands with atoms at van der Waals radii; **DD**, **EE**, **FF**, analogous views of the nonhelical complex.

As would be expected from the shorter sp^3 carbon chains, **7**·(toluene)$_4$ and **7**·$(CHCl_3)_2$ crystallized in nonhelical conformations. The sp^3 chains of the former laterally shielded the sp chain, whereas those of the latter bowed in similar directions, exposing more of the sp chain. The average sp/sp^3 distance in the former (3.932 Å) was shorter than that in the double-helical complexes; that in the latter (3.989 Å) was comparable to the double-helical complexes. However, **7**·$(CHCl_3)_2$ was more dense (1.616 vs 1.468 Mg/m^3), likely due in part to the heavier solvate molecule. In **9**·$(CH_2Cl_2)_{2.5}$, the longer sp^3 chains also bowed in similar directions, with a somewhat greater average sp/sp^3 distance (4.090 Å).

The dodecahexaynediyl complex **11**·$(CH_2Cl_2)_{0.67}$ exhibited two independent molecules in the unit cell (2:1 ratio). As shown in Figure 6, the dominant form showed a double-helical conformation (**AA**−**CC**). However, it was less twisted than the others, with an angle of 163.2° between the P−Pt−P/Pt planes and a helix pitch of 39.76 Å. Hence, the sp carbon chain is much less shielded than with the octatetraynediyl complexes in Figures 1−3. The second form was nonhelical (**DD**−**FF**), with an average sp/sp^3 distance much greater than that of the helical form (4.157 vs 3.868 Å). Metrical data for the first are given in Table 1, and those for the second are presented in Table 2. From these results, we propose that an sp^3/sp carbon ratio of at least 1.50 is required for a helical conformation.

5. Dynamic and Redox Properties. For each of the above molecules that could reasonably be expected to adopt a double-helical conformation, a confirmatory crystal structure has been obtained. Thus, even though **5** and **11** can also crystallize in nonhelical conformations, we thought it likely that helical motifs would be favored in solution and not solely imposed by crystal lattices. Helical molecules often contain diastereotopic groups, such as the PAr_2 substituents in **3**−**5**. In solution, separate NMR signals are frequently observed.[4b] However, when the helix can

Table 4. Cyclic Voltammetry Data

complex[a]	$E_{p,a}$ [V]	$E_{p,c}$ [V]	E° [V]	ΔE [mV]	$i_{c/a}$
2[b]	1.261	1.143	1.202	118	0.48
3	1.306	1.224	1.265	82	0.78
4	1.259	1.168	1.214	91	0.71
5	1.249	1.156	1.203	93	0.76
7	1.315	1.179	1.247	136	0.10
8	1.326	1.241	1.284	85	0.36
10[b]	1.467[b]	1.306	1.387	161	-
11	1.465	1.372	1.418	93	0.35
6	1.301	1.214	1.258	87	0.68

[a] Conditions: $(7-9) \times 10^{-4}$ M, *n*-Bu_4N^+ BF_4^-/CH_2Cl_2 at 22.5 ± 1 °C; Pt working and counter electrodes, potential vs Ag wire pseudoreference; scan rate 100 mV s^{-1}; ferrocene = 0.46 V. [b]Data from ref 14a.

"untwist" and rewind to an enantiomer, net exchange occurs. When this is rapid on the NMR time scale, only a single signal is observed.

Room-temperature NMR spectra of **3**−**5** showed only a single signal for all potentially diastereotopic atoms or groups. Thus, numerous low-temperature spectra were recorded, some of which are depicted elsewhere.[26b] However, even at the lowest feasible temperatures, separate signals could not be observed (**3**, CD_2Cl_2 (−40 °C; solubility limit), toluene-d_8 (−90 °C; ^{13}C signals *i*/*p* to P); **4**, THF-d_8 (−120 °C; ^{13}C signals *i*/*p* to P; CH_3 ^1H and ^{13}C signals); **5**, THF-d_8 (−120 °C; ^{13}C signals *i*/*p* to P; $C(CH_3)_3$ ^1H and ^{13}C signals). As analyzed further below, we interpret this as indicating a low barrier, ≤12 kcal/mol, for interconverting enantiomeric double helices.

In order to characterize the redox properties of the preceding complexes, cyclic voltammograms were recorded in CH_2Cl_2. The conditions were identical to those used previously for diplatinum complexes such as **2** and **10**.[14a] Data are summarized in Table 4, and typical traces are compared in Figure 7.

Oxidations, presumably to the corresponding mixed-valent radical cations,[22] were always observed, but no reductions took place prior to the solvent-induced limit.[37] Although the oxidations were not chemically or electrochemically reversible, the degree of reversibility, as reflected by the $i_{c/a}$ and ΔE values, was greater for the helical complexes. This is readily seen in the pairs of traces in Figure 7. Although the anodic currents for **3** and **4** are less than or equal to those of the nonhelical model compounds **6** and **2**, their cathodic currents are significantly greater, indicative of longer-lived radical cations.

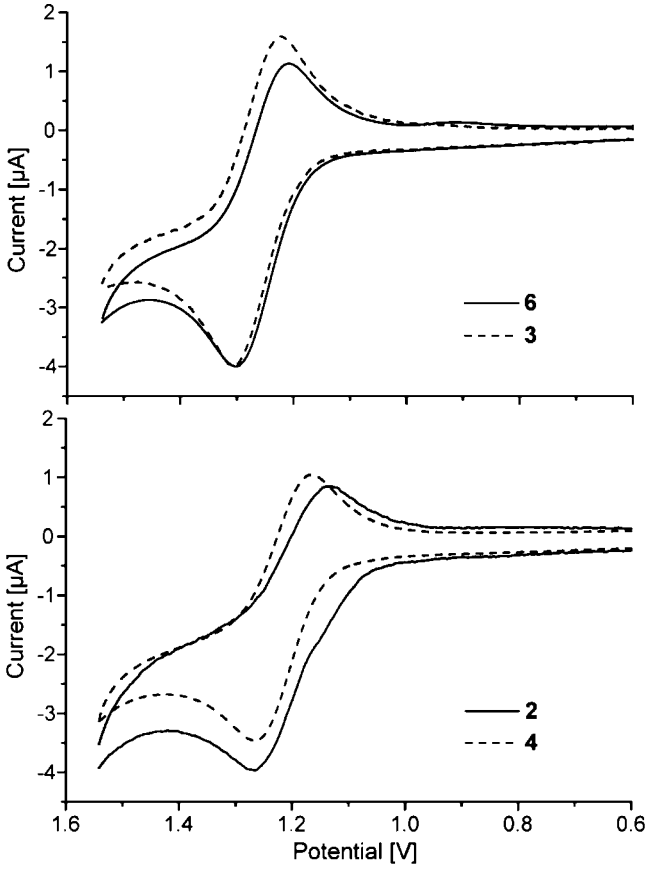

Figure 7. Comparison of the cyclic voltammograms of double-helical complexes **3** and **4** with those of model compounds **6** and **2**.

Discussion

1. Syntheses. Our route to the title molecules (Schemes 4, 5) can be viewed as a one-dimensional analogue of the coordination-driven self-assembly processes used by Stang and Fujita to access two- and three-dimensional polypalladium and polyplatinum complexes with other types of rigid spacers.[38] However, as noted above, success is capricious. In some cases, oligomerization appears to be competitive; in other cases, the target molecules appear to form but oligomerize upon attempted workup. As described in the following paper,[24] many complexes that cannot be accessed are easily prepared by the alternative route in Scheme 2, using alkene metathesis/hydrogenation sequences. The resulting samples show no tendency to oligomerize.

It is also not obvious why systems with *p*-tolyl-substituted platinum endgroups (**1**, Scheme 3) are more disposed toward oligomerization than those with pentafluorophenyl-substituted end groups (**2**, **10**; Schemes 4, 5). This may reflect subtle differences in the relative rate constants for the initial phosphine substitution step and the rate-determining step for oligomerization. However, deeper insight will require mechanistic investigations beyond the scope of this study. The use of P*p*-tol_3 ligands in **2** and **10** as opposed to the PPh_3 ligands in **1** gives somewhat more soluble educts, in which the phosphines remain weakly basic enough to be displaced by the monophosphine PPh_2(*n*-octyl) (leading to **6**)[30] and the electronically similar diphosphines $Ph_2P(CH_2)_mPPh_2$.

In principle, the reactions in Schemes 3−5 could also give isomers of the type **H′** (Scheme 2), which contain *trans*-spanning diphosphine ligands. However, attempts to generate similar monoplatinum species via substitution reactions proceed in very low yields and give much oligomer.[34] Authentic samples have been synthesized by another route[24] and do not readily equilibrate with the title molecules.

2. Spectroscopic and Redox Properties. The IR and UV−visible spectra of diplatinum polyynediyl complexes *trans*,*trans*-$(Ar')(Ar_3P)_2Pt(C{\equiv}C)_nPt(PAr_3)_2(Ar')$ have been extensively analyzed in previous papers.[14] As noted above, the termini-spanning diphosphine ligands in **3**−**9** and **11** have no detectable effect. Given the magnetic anisotropy and deshielding effects that

(37) Reduction of the $Pt(C{\equiv}C)_8Pt$ homologue of **2** and **10** can be observed in THF, which has a wider cathodic window. However, species with shorter sp carbon chains exhibit no reduction.

(38) (a) Leininger, S.; Olenyuk, B.; Stang, P. J. *Chem. Rev.* **2000**, *100*, 853. (b) Fujita, M.; Tominaga, M.; Hori, A.; Therrien, B. *Acc. Chem. Res.* **2005**, *38*, 369.

Scheme 6. Conformational Changes Required for the Interconversion of Enantiomers of the Double-Helical Complexes

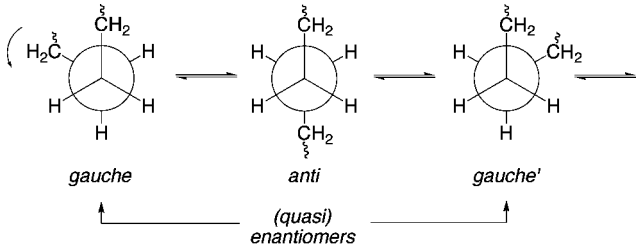

characterize C≡C linkages,[39] we had thought that NMR chemical shifts of the sp^3 carbon chains might reflect average distances from the sp carbon chain. However, DFT calculations show that when an sp^3 carbon atom is moved from 3.5 Å to 5.5 Å away from the midpoint of an octatetrayne in a perpendicular plane, the ^{13}C NMR chemical shift varies negligibly.[40]

The thermal stabilities of **3**−**9** and **11** are also comparable to analogues without termini-spanning diphosphine ligands. However, the redox properties show several interpretable differences. Oxidations of other diplatinum(II) complexes with bridging unsaturated ligands afford mixed valent platinum(II)/platinum(III) radical cations.[22] Furthermore, there is good evidence that platinum(III) species often decompose via solvent interaction with the vacant axial coordination site. Stabilities are enhanced when the axial position is sterically shielded.[22] Importantly, the sp^3 carbon chains in the title molecules markedly increase axial shielding (compare **Q** and **S** vs **M** in Figure 3).

Consider the cyclic voltammetry data for **3** in Table 4. It undergoes the most reversible oxidation of the $Pt(C{\equiv}C)_4Pt$ complexes, as reflected by the $i_{c/a}$ and ΔE values. Complexes **4** and **5** are comparable; their $E°$ values are slightly less positive, indicating thermodynamically more favorable oxidations, consistent with the electron-releasing *p*-alkyl PAr_2 substituents. In going from **3** to **6**, the sp^3 chains are replaced by *n*-octyl groups, making the sp carbon chains and axial positions on platinum more accessible. The $E°$ values of **3** and **6** are quite close (1.265 vs 1.258 V), but the ΔE and $i_{c/a}$ values (82 vs 87 mV; 0.78 vs 0.68) indicate a loss of reversibility, as highlighted in the overlaid traces in Figure 7 (top).

In going from **4** to **2**, the sp^3 chains are replaced by *p*-tolyl substituents. The ΔE and $i_{c/a}$ values (91 vs 118 mV; 0.71 vs 0.48) now indicate a substantial loss of reversibility (see Figure 7, bottom). In **7** and **8**, the shorter sp^3 chains do not shield the $Pt(C{\equiv}C)_4Pt$ moiety as extensively. Also, some ring strain may be introduced. Accordingly, reversibilities drop dramatically ($i_{c/a}$ 0.10 and 0.36). In accord with MO analyses,[41] complexes with longer sp chains are thermodynamically more difficult to oxidize[14,16] and furthermore show much poorer reversibilities. Both trends are evident with the $Pt(C{\equiv}C)_6Pt$ complexes **10** and **11**. However, the sterically shielded complex again exhibits superior reversibility.

3. Crystal Structures. Of the structural features described above, the conformations of the $CH_2CH_2CH_2CH_2$ and CH_2CH_2-CH_2PAr_2 moieties are particularly deserving of further analysis. As illustrated in Scheme 6, gauche and anti geometries are possible; the former are chiral. Although there are other types of chiral conformational moieties in the title molecules, the helical chirality is derived from these gauche segments. In order for the enantiomers to interconvert, each gauche segment must invert. One would expect the lowest energy pathway to involve "untwisting" to an anti conformation and then continued twisting to a gauche conformation of the opposite chirality. Only in complexes with longer sp^3 chains would "belt-tightening" syn transition states be conceivable.

One question is whether there are any "conserved regions" in the $Pt(C{\equiv}C)_4Pt$ complexes with $Ar_2P(CH_2)_{14}PAr_2$ bridges. As noted above and reflected by the torsion angles in Table 3, the structures of **3**·$(benzene)_{1.5}$ and **3**·$(toluene)_{1.5}$ are very similar. One sp^3 chain exhibits an identical pattern of four gauche and nine anti segments (angles given on left). The other exhibits three mismatches, with three and four gauche segments, respectively. In neither molecule are the gauche/anti patterns of the two sp^3 chains identical or symmetrical about the midpoint. In contrast, the sp^3 chains of **5**·$(toluene)_{5.5}$ exhibit identical patterns (four gauche, nine anti) that are symmetrical about the midpoint. The sp^3 chains in **4** are very similar, with just one anti/gauche mismatch.

All of the $CH_2CH_2CH_2PAr_2$ segments in these four molecules exhibit anti conformations, which avoid 1,5-synperiplanar interactions[42] with PAr_2 groups. With a single exception, the immediately adjacent $CH_2CH_2CH_2CH_2$ segments exhibit gauche conformations, representing the onset of helicity. In **4** and **5**·$(toluene)_{5.5}$, the anti $CH_2CH_2CH_2CH_2$ segments are grouped in the middle of the chain, leading to the motif evident in **S** in Figure 3. In all of the sp^3 chains except one of **3**·$(benzene)_{1.5}$, the gauche torsion angles have the same sign, indicating the same helical chirality.

In the nonhelical structure **5**·$(toluene)_2$, the sp^3 chain must connect two phosphorus atoms that are syn as opposed to anti. Hence, the distance that must be spanned is shorter. Accordingly, the sp^3 chains in **5**·$(toluene)_2$ are more kinked, with five gauche segments each. Since this structure has a center of symmetry, the chains are identical, but the gauche segments are asymmetrically distributed. In the nonhelical complexes with shorter sp^3 chains (Figure 5), the distances that must be spanned per methylene group are greater. All exhibit fewer gauche segments; in the nondisordered structure **7**·$(CHCl_3)$, there is only one in each chain (Table s2, Supporting Information).

In both the helical and nonhelical molecules in **11**·$(CH_2Cl_2)_{0.67}$, the $CH_2CH_2CH_2PAr_2$ and immediately adjacent $CH_2CH_2CH_2CH_2$ segments exhibit anti and gauche conformations, respectively. Each sp^3 chain features 10−12 anti and 5−7 gauche conformations, the latter of both signs, as tabulated in the Supporting Information. In one sp^3 chain of the helical form, the pattern is symmetrical about the midpoint; the other contains two mismatches. There is no discernible pattern in the nonhelical form, in which the chains are symmetry equivalent. Although the angle defined by the P−Pt−P/Pt planes in the helical form (163.2°) is only ca. 15% less than that with **3**−**5**, the much greater platinum−platinum distance results in a much longer helix pitch (39.76 vs 23.66−24.45 Å).

4. Solution Structures and Dynamic Properties. The crystallographic data for the $Pt(C{\equiv}C)_4Pt$ complexes with $Ar_2P(CH_2)_{14}PAr_2$ bridges suggest that they exist as equilibrium

(39) Wannere, C. S.; Schleyer, P. v. R. *Org. Lett.* **2003**, *5*, 605.
(40) Jiao, H. Unpublished results, Universität Erlangen-Nürnberg.
(41) Zhuravlev, F.; Gladysz, J. A. *Chem.—Eur. J.* **2004**, *10*, 6510.
(42) Hoffmann, R. W. *Angew. Chem., Int. Ed.* **2000**, *39*, 2054; *Angew. Chem.* **2000**, *112*, 2134.

mixtures of at least several chiral double-helical and formally achiral nonhelical conformations in solution. As analyzed above and below, we believe that the former should dominate. However, we have been unable to establish a chiral ground state, which would feature diastereotopic aryl groups, by low-temperature NMR. This in turn raises several questions.

First, might the double-helical conformations in Figures 1−3 reflect some deep-seated lattice packing preference? For example, diplatinum polyynediyl complexes *trans,trans*-(X)(R_3P)$_2$Pt(C≡C)$_n$Pt(PR_3)$_2$(X) ($n \geq 3$; R = alkyl, Ar; X = Ar′, Cl) always crystallize with essentially coplanar endgroups,[14,25b,43] even though DFT calculations show no electronic driving force.[41] Since a packing driving force would be difficult to prove, we have focused on structural modifications that might raise the barrier for interconverting enantiomeric helical ground states.

Several components to this barrier can be identified. First, as noted above, there are torsional motions involving the CH_2-$CH_2CH_2PAr_2$ and $CH_2CH_2CH_2CH_2$ segments and other portions of the molecule. These would occur both sequentially and in concert. The activation energy for the conversion of gauche- to anti-butane (see Scheme 6) is ca. 2.7 kcal/mol. If the rate-determining step featured one such energy maximum in each sp^3 chain, the conformation of which would logically be derived from a local minimum higher than the ground state, the barrier should significantly surpass 5.4 kcal/mol. Second, there should be attractive van der Waals and possibly CH/π interactions between the sp and sp^3 chains. These should be maximized in helical conformations and diminished in the transition state for the rate-determining step.

Thus, higher barriers would be expected for complexes with longer sp and sp^3 chains, which should have greater van der Waals contact surfaces. This possibility is explored in the following paper.[24] Another approach would be to decrease the sp chain length, such that endgroup−endgroup interactions destabilize the achiral planar ground state, analogous to the situation in ortho-substituted biaryls. Efforts in this direction have also been initiated.[25b] Alternatively, functional groups could be introduced on the sp^3 chain, which might enhance attractive interactions with the sp chain. Recently, similar complexes with ethereal diphosphines have been reported.[44]

The gain that might be associated with the first strategy is illustrated by data of Moore. He measured the binding energies of rodlike guests in the inner cavities of single-helical foldamer hosts.[45] These increased with increasing lengths of the hosts, up to the point where that of the guest molecule was exceeded. Nonetheless, none of these approaches or others[46] have yet led to a complex for which a chiral ground state can be demonstrated. Hence, the dominant conformation of the title molecules in solution remains an unsettled question.

5. Further Analyses of Helicity. The preceding issues aside, the title molecules are unique in the *absence* of bonding interactions or complementarity between the two helical chains. The sp carbon chain provides a mechanical support, without which the helical conformation would not be energetically competitive in solution or the solid state. Although the comparison is unflattering in the nanotechnology era, our complexes can be viewed as molecular analogues of beanpoles, implements used by the most ancient agrarian societies to template upwardly spiraling vines.

Comparable molecules are challenging to identify. Distant relatives would include biphenyls in which the *o*/*o* and *o*′/*o*′ positions are bridged by sp^3 carbon chains. Systems with as many as four methylene groups have been described.[47] However, the helix strands are splayed outward from the biphenyl axis. Future studies of "*carbo*-mer" or (C≡C)-expanded analogues[48] would be worthwhile and may yield structures resembling those in Figures 1−3.

There is an extensive literature of single helical molecules,[1] some of which are particularly relevant to the title molecules. Rebek has demonstrated that when guests with longer $(CH_2)_m$ segments bind within cavitands or container molecules of appropriate diameters and/or lengths, helical conformations are induced.[49] This can be viewed as an "external" templating, in contrast to our "internal" beanpole template. Both we and Hirsch have prepared polyynes in which the termini are joined by a single $(CH_2)_m$ tether.[50,51] However, no structural data are so far available.

Although we could not obtain barriers for the interconversion of the enantiomers of the helical molecules in Figures 1−3, the values would represent a measure of the sp carbon chain protection, analogous to the way insulation for electrical wire is graded. A correlation to the extra activation energy required for attack upon the sp carbon chains, versus model compounds such as **6**, would be expected. However, from the standpoint of engineering functional molecular devices, a portfolio of flexible bridges with a gradation of barriers would be optimal.

6. Conclusion

This study has demonstrated the accessibility of an unprecedented new class of double-helical molecules in which two sp^3 carbon chains wrap around an sp carbon chain via a one-step coordination-driven self-assembly process. In contrast to other double-helical molecules, there is an absence of bonding interactions or complementarity between the strands. There are, however, synergies between the chains. The sp chain provides a mechanical support, without which helical conformations would not be energetically competitive. The sp^3 chain in turn serves as a protecting group, enhancing the stabilities of mixed-valent radical cations. There is an obvious analogy to household insulated wire. Alternative routes to this class of molecules, and a variety of isomers and derivatives, will be detailed in upcoming full papers.[24,44b]

(43) Zheng, Q.; Hampel, F.; Gladysz, J. A. *Organometallics* **2004**, *23*, 5896.
(44) (a) de Quadras, L.; Hampel, F.; Gladysz, J. A. *Dalton Trans.* **2006**, 2929. (b) de Quadras, L.; Bauer, E. B.; Stahl, J.; Zhuravlev, F.; Hampel, F.; Gladysz, J. A. *New J. Chem.* **2007**. Manuscript submitted for publication.
(45) (a) Tanatani, A.; Mio, M. J.; Moore, J. S. *J. Am. Chem. Soc.* **2001**, *123*, 1792. (b) Stone, M. T.; Heemstra, J. M.; Moore, J. S. *Acc. Chem. Res.* **2006**, *39*, 11.
(46) Helical structures might have greater inversion barriers in more polar solvents. However, these tend to have higher freezing points, hampering low temperature measurements. Also, since a positive $\Delta V^{\ddagger}$ value would be expected, rates should slow under pressure.
(47) Müllen, K.; Heinz, W.; Klärner, F.-G.; Roth, W. R.; Kindermann, I.; Adamczak, O.; Wette, M.; Lex, J. *Chem. Ber.* **1990**, *123*, 2349.
(48) Maraval, V.; Chauvin, R. *Chem. Rev.* **2006**, *106*, 5317.
(49) (a) Trembleau, L.; Rebek, J., Jr. *Science* **2003**, *301*, 1219. (b) Scarso, A.; Trembleau, L.; Rebek, J., Jr. *Angew. Chem., Int. Ed.* **2003**, *42*, 5499; *Angew. Chem.* **2003**, *115*, 5657.
(50) (a) Horn, C. R.; Martín-Alvarez, J. M.; Gladysz, J. A. *Organometallics* **2002**, *21*, 5386. (b) Horn, C. R.; Gladysz, J. A. *Eur. J. Inorg. Chem.* **2003**, *9*, 2211.
(51) Klinger, C.; Vostrowsky, O.; Hirsch, A. *Eur. J. Org. Chem.* **2006**, 1508.

Experimental Section

***trans,trans*-(C$_6$F$_5$)(Ph$_2$P(CH$_2$)$_{14}$PPh$_2$)Pt(C≡C)$_4$Pt(Ph$_2$P(CH$_2$)$_{14}$PPh$_2$)(C$_6$F$_5$) (3).** A Schlenk flask was charged with *trans,trans*-(C$_6$F$_5$)(*p*-tol$_3$P)$_2$Pt(C≡C)$_4$Pt(P*p*-tol$_3$)$_2$(C$_6$F$_5$) (**2**;[14a] 0.204 g, 0.100 mmol) and CH_2Cl_2 (40 mL). A solution of $Ph_2P(CH_2)_{14}PPh_2$ (0.150 g, 0.265 mmol)[27] in CH_2Cl_2 (20 mL) was passed through a 2 cm silica gel pad directly into the Schlenk flask with stirring. After 2 h, the solvent was removed by oil pump vacuum, and ethanol (30 mL) was added. The yellow solid was collected by filtration, washed with ethanol (2 × 10 mL), and dried by oil pump vacuum to give **3** (0.170 g, 0.087 mmol, 87%), mp >245 °C dec. Calcd for $C_{96}H_{96}F_{10}P_4Pt_2$: C, 59.01; H, 4.95. Found: C, 59.48; H, 5.27. DSC: endotherm with T_i, 181.6 °C; T_e, 244.0 °C; T_p, 263.7 °C; T_c, 270.3 °C; T_f, 270.2 °C; exotherm with T_i, 271.0 °C.[52] TGA: onset of mass loss (T_i), 286.0 °C.

NMR (δ, $CDCl_3$) ^{1}H 7.40 (m, 16H of 8 Ph), 7.28 (m, 8H of 8 Ph), 7.19 (m, 16H of 8 Ph), 2.68 (m, 8H, PCH_2), 2.15 (m, 8H, PCH_2CH_2), 1.63−1.47 (m, 8H, $PCH_2CH_2CH_2$), 1.46−1.22 (m, 32H, remaining CH_2); ^{13}C{^{1}H}[53,54] 145.6 (dd, $^1J_{CF}$ = 223 Hz, $^2J_{CF}$ = 22 Hz, *o* to Pt), 136.3 (dm, $^1J_{CF}$ = 240 Hz, *m*/*p* to Pt), 132.8 (virtual t, $^2J_{CP}$ = 5.7 Hz, *o* to P), 132.0 (virtual t, $^1J_{CP}$ = 27.9 Hz, *i* to P), 130.1 (s, *p* to P), 127.8 (virtual t, $^3J_{CP}$ = 5.0 Hz, *m* to P), 98.6 (s, $^1J_{CPt}$ = 960 Hz,[55] PtC≡), 94.2 (s, $^2J_{CPt}$ = 266 Hz,[55] PtC≡*C*), 63.4 (s, PtC≡C*C*), 57.9 (s, PtC≡CC≡*C*), 30.6 (virtual t, $^3J_{CP}$ = 8.0 Hz, $PCH_2CH_2CH_2$), 30.0 (s, CH_2), 29.5 (s, CH_2), 29.3 (s, CH_2), 28.1 (virtual t, $^1J_{CP}$ = 18.3 Hz, PCH_2), 28.0 (s, CH_2), 25.6 (s, PCH_2CH_2); ^{31}P{^{1}H} 14.9 (s, $^1J_{PPt}$ = 2582 Hz).[55] IR (cm^{-1}, powder film): $\nu_{C\equiv C}$ 2148 (m), 2007 (w). UV−vis:[56] 265 (72 800), 291 (86 000), 318 (109 000), 353 (7200), 379 (4800), 412 (2400). MS:[57] 1954 (**3**$^+$, 100%), 1784 ([**3**−C$_6$F$_5$−H$_2$]$^+$, 2%), no other significant peaks >1300.

***trans,trans*-(C$_6$F$_5$)(*p*-tol$_2$P(CH$_2$)$_{14}$P*p*-tol$_2$)Pt(C≡C)$_4$Pt(*p*-tol$_2$P(CH$_2$)$_{14}$P*p*-tol$_2$)(C$_6$F$_5$) (4).** Complex **2** (0.153 g, 0.075 mmol), CH_2Cl_2 (40 mL), and a solution of *p*-tol$_2$P(CH$_2$)$_{14}$P*p*-tol$_2$ (0.120 g, 0.120 mmol)[30] in CH_2Cl_2 (20 mL) were combined in a procedure analogous to that for **3**. An identical workup gave **4** as a yellow solid (0.140 g, 0.068 mmol, 91%), mp >210 °C dec. Calcd for $C_{104}H_{112}F_{10}P_4Pt_2$: C, 60.46; H, 5.46. Found: C, 60.42; H, 5.60. DSC: endotherm with T_i, 196.2 °C; T_e, 213.2 °C; T_p, 242.2 °C; T_c, 255.6 °C; T_f, 259.3 °C; exotherm with T_i, 260.0 °C.[52] TGA: onset of mass loss (T_i), 260.3 °C.

NMR (δ, $CDCl_3$) ^{1}H 7.27 (m, 16H, *o* to P), 6.99 (m, 16H, *m* to P), 2.63 (m, 8H, PCH_2), 2.29 (s, 24H, CH_3), 2.10 (m, 8H, PCH_2CH_2), 1.60−1.47 (m, 8H, $PCH_2CH_2CH_2$), 1.46−1.21 (m, 32H, remaining CH_2); ^{13}C{^{1}H}[53,54] 145.7 (dd, $^1J_{CF}$ = 222 Hz, $^2J_{CF}$ = 22 Hz, *o* to Pt), 140.3 (s, *p* to P), 136.3 (dm, $^1J_{CF}$ = 250 Hz, *m*/*p* to Pt), 132.8 (virtual t, $^2J_{CP}$ = 6.0 Hz, *o* to P), 128.7 (virtual t, $^1J_{CP}$ = 29.4 Hz, *i* to P), 128.5 (virtual t, $^3J_{CP}$ = 5.5 Hz, *m* to P), 99.2 (s, PtC≡), 94.1 (s, $^2J_{CPt}$ = 269 Hz, PtC≡*C*), 63.5 (s, PtC≡C*C*), 57.8 (s, PtC≡CC≡*C*), 30.7 (virtual t, $^3J_{CP}$ = 7.8 Hz, $PCH_2CH_2CH_2$), 30.0 (s, CH_2), 29.6 (s, CH_2), 29.4 (s, CH_2), 28.3 (virtual t, $^1J_{CP}$ = 18.4 Hz, PCH_2), 28.0 (s, CH_2), 25.5 (s, PCH_2CH_2), 21.2 (s, CH_3); ^{31}P{^{1}H} 13.5 (s, $^1J_{PPt}$ = 2562 Hz).[55] IR (cm^{-1}, powder film): $\nu_{C\equiv C}$ 2146 (m), 2003 (w). MS:[57] 2066 (**4**$^+$, 100%), 1973 ([**4**−C$_6$F$_5$−H$_2$]$^+$, 2%), 1897 ([**4**−2C$_6$F$_5$−H$_2$]$^+$, 4%), no other significant peaks >850.

***trans,trans*-(C$_6$F$_5$)((*p*-*t*-BuC$_6$H$_4$)$_2$P(CH$_2$)$_{14}$P(*p*-C$_6$H$_4$-*t*-Bu)$_2$)Pt(C≡C)$_4$Pt((*p*-*t*-BuC$_6$H$_4$)$_2$P(CH$_2$)$_{14}$P(*p*-C$_6$H$_4$-*t*-Bu)$_2$)(C$_6$F$_5$) (5).** Complex **2** (0.153 g, 0.075 mmol), CH_2Cl_2 (50 mL), and a solution of (*p*-*t*-BuC$_6$H$_4$)$_2$P(CH$_2$)$_{14}$P(*p*-C$_6$H$_4$-*t*-Bu)$_2$ (0.149 g, 0.188 mmol)[30] in CH_2Cl_2 (94 mL) were combined in a procedure analogous to that for **3**. An identical workup gave **5** as a yellow solid (0.138 g, 0.057 mmol, 77%), mp >210 °C dec. Calcd for $C_{128}H_{160}F_{10}P_4Pt_2$: C, 63.99; H, 6.71. Found: C, 64.72; H, 6.92.

NMR (δ, $CDCl_3$) ^{1}H 7.30 (m, 16H, *o* to P), 7.17 (m, 16H, *m* to P), 2.61 (m, 8H, PCH_2), 2.20 (m, 8H, PCH_2CH_2), 1.63−1.49 (m, 8H, $PCH_2CH_2CH_2$), 1.46−1.25 (m, 32H, remaining CH_2), 1.23 (s, 72H, CH_3); ^{13}C{^{1}H}[53,54] 153.3 (s, *p* to P), 145.5 (dd, $^1J_{CF}$ = 224 Hz, $^2J_{CF}$ = 24 Hz, *o* to Pt), 136.0 (dm, $^1J_{CF}$ = 248 Hz, *m*/*p* to Pt), 132.6 (virtual t, $^2J_{CP}$ = 5.8 Hz, *o* to P), 128.8 (virtual t, $^1J_{CP}$ = 28.7 Hz, *i* to P), 124.7 (virtual t, $^3J_{CP}$ = 5.1 Hz, *m* to P), 99.1 (s, PtC≡), 94.4 (s, PtC≡*C*), 63.7 (s, PtC≡C*C*), 57.5 (s, PtC≡CC≡*C*), 34.7 (s, *C*(CH$_3$)$_3$), 31.1 (s, CH_3), 30.6 (virtual t, $^3J_{CP}$ = 7.9 Hz, $PCH_2CH_2CH_2$), 30.4 (s, CH_2), 29.9 (s, CH_2), 29.5 (s, CH_2), 28.3 (virtual t, $^1J_{CP}$ = 18.3 Hz, PCH_2), 27.9 (s, CH_2), 25.7 (s, PCH_2CH_2); ^{31}P{^{1}H} 12.7 (s, $^1J_{PPt}$ = 2561 Hz).[55] IR (cm^{-1}, powder film): $\nu_{C\equiv C}$ 2146 (m), 2003 (w). UV−vis:[56] 292 (114 000), 318 (154 000), 351 (8000), 379 (8000), 410 (4000). MS:[57] 2402 (**5**$^+$, 100%), no other significant peaks >975.

***trans,trans*-(C$_6$F$_5$)(Ph$_2$P(CH$_2$)$_{10}$PPh$_2$)Pt(C≡C)$_4$Pt(Ph$_2$P(CH$_2$)$_{10}$PPh$_2$)(C$_6$F$_5$) (7).** Complex **2** (0.153 g, 0.075 mmol), CH_2Cl_2 (75 mL), and a solution of $Ph_2P(CH_2)_{10}PPh_2$ (0.093 g, 0.180 mmol)[27,28] in CH_2Cl_2 (180 mL) were combined in a procedure analogous to that for **3**. An identical workup gave **7** as a yellow solid (0.111 g, 0.060 mmol, 80%), mp >200 °C dec. DSC: endotherm with T_i, 222.9 °C; T_e, 258.1 °C; T_p, 271.5 °C; T_c, 279.1 °C; T_f, 278.9 °C; exotherm with T_i, 279.1 °C.[52] TGA: onset of mass loss (T_i), 264 °C.

NMR (δ, $CDCl_3$) ^{1}H 7.38 (m, 16H of 8 Ph), 7.29 (m, 8H of 8 Ph), 7.21 (m, 16H of 8 Ph), 2.71 (m, 8H, PCH_2), 2.01 (m, 8H, PCH_2CH_2), 1.58−1.47 (m, 8H, $PCH_2CH_2CH_2$), 1.40−1.25 (m, 16H, remaining CH_2); ^{13}C{^{1}H}[53,54] 145.8 (d, $^1J_{CF}$ = 227 Hz, *o* to Pt), 136.4 (dm, $^1J_{CF}$ = 239 Hz, *m*/*p* to Pt), 132.8 (virtual t, $^2J_{CP}$ = 5.8 Hz, *o* to P), 131.9 (virtual t, $^1J_{CP}$ = 27.5 Hz, *i* to P), 130.3 (s, *p* to P), 127.9 (virtual t, $^3J_{CP}$ = 5.1 Hz, *m* to P), 101.6 (s, PtC≡), 94.0 (s, PtC≡*C*), 64.4 (s, PtC≡C*C*), 59.3 (s, PtC≡CC≡*C*), 32.2 (virtual t, $^3J_{CP}$ = 7.6 Hz, $PCH_2CH_2CH_2$), 30.7 (s, CH_2), 29.9 (s, CH_2), 29.2 (virtual t, $^1J_{CP}$ = 18.3 Hz, PCH_2), 26.4 (s, PCH_2CH_2); ^{31}P{^{1}H} 14.4 (s, $^1J_{PPt}$ = 2572 Hz).[55] IR (cm^{-1}, powder film): $\nu_{C\equiv C}$ 2138 (m), 1996 (w). MS:[57] 1841 (**7**$^+$, 100%), 1763 ([**7**−C$_6$H$_5$−H]$^+$, 2%), 1673 ([**7**−C$_6$F$_5$−H]$^+$, 4%), no other significant peaks >900.

***trans,trans*-(C$_6$F$_5$)(Ph$_2$P(CH$_2$)$_{11}$PPh$_2$)Pt(C≡C)$_4$Pt(Ph$_2$P(CH$_2$)$_{11}$PPh$_2$)(C$_6$F$_5$) (8).** Complex **2** (0.153 g, 0.075 mmol), CH_2Cl_2 (75 mL), and a solution of $Ph_2P(CH_2)_{11}PPh_2$ (0.094 g, 0.180 mmol)[27,28] in CH_2Cl_2 (180 mL) were combined in a procedure analogous to that for **3**. An identical workup gave **8** as a yellow solid (0.113 g, 0.060 mmol, 80%), mp >220 °C dec. DSC: endotherm with T_i, 188.5 °C; T_e, 225.1 °C; T_p, 244.1 °C; T_c, 251.8 °C; T_f, 254.1 °C; exotherm with T_i, 256 °C.[52] TGA: onset of mass loss (T_i) 267 °C.

NMR (δ, $CDCl_3$) ^{1}H 7.39 (m, 16H of 8 Ph), 7.29 (m, 8H of 8 Ph), 7.21 (m, 16H of 8 Ph), 2.71 (m, 8H, PCH_2), 2.09 (m, 8H, PCH_2CH_2), 1.56−1.23 (m, 28H, remaining CH_2); ^{13}C{^{1}H}[53,54] 145.8 (d, $^1J_{CF}$ = 228 Hz, *o* to Pt), 136.4 (dm, $^1J_{CF}$ = 247 Hz, *m*/*p* to Pt), 132.9 (virtual t, $^2J_{CP}$ = 5.6 Hz, *o* to P), 131.9 (virtual t, $^1J_{CP}$ = 27.7 Hz, *i* to P), 130.3

(52) (a) DSC and TGA data were treated as recommended by Cammenga, H. K.; Epple, M. *Angew. Chem., Int. Ed. Engl.* **1995**, *34*, 1171; *Angew. Chem.* **1995**, *107*, 1284. The T_e values best represent the temperature of the phase transition or exotherm. (b) Except in cases of desolvation, DSC measurements were not continued beyond the onset of mass loss (TGA).

(53) (a) In most ^{13}C NMR spectra, the *i*-C$_6$F$_5$ signal was not observed. (b) For virtual triplets (Hersh, W. H. *J. Chem. Educ.* **1997**, *74*, 1485), the *J* values represent the *apparent* couplings between adjacent peaks. (c) The PtC≡CC≡C signals were assigned according to trends established earlier.[14]

(54) Complexes with PtPCH$_2$CH$_2$CH$_2$ linkages exhibit a characteristic pattern of ^{13}C NMR signals. A ^{1}H,^{1}H COSY spectrum of **4** was used to make definitive assignments of the corresponding ^{1}H signals, and a ^{1}H,^{13}C COSY spectrum in turn gave definitive assignments of the ^{13}C signals. Analogous experiments have been conducted with closely related compounds.[34]

(55) This coupling represents a satellite (d; ^{195}Pt = 33.8%) and is not reflected in the peak multiplicity given.

(56) UV−visible spectra were recorded in CH_2Cl_2 (1.25×10^{-6} M). Absorptions are in nm (ϵ, M^{-1} cm^{-1}).

(57) FAB (3-nitrobenzyl alcohol matrix); *m*/*z* for the most intense peak of the isotope envelope.

(58) Additional data are available from the Cambridge Crystallographic Data Centre via the following CCDC numbers: 171482 (**3**·(toluene)$_{1.5}$), 176209 (**3**·(benzene)$_{1.5}$), 171483 (**4**), 171486 (**5**·(toluene)$_{5.5}$), 606935 (**5**·(toluene)$_2$), 171485 (**7**·(toluene)$_4$), 171484 (**7**·(CHCl$_3$)$_2$), 606936 (**9**·(CH$_2$Cl$_2$)$_{2.5}$), 171481 (**11**·(CH$_2$Cl$_2$)$_{0.67}$).

(s, *p* to P), 127.9 (virtual t, $^3J_{CP}$ = 5.1 Hz, *m* to P), 99.4 (s, PtC≡), 93.7 (s, PtC≡*C*), 63.4 (s, PtC≡C*C*), 58.5 (s, PtC≡CC≡*C*), 31.3 (virtual t, $^3J_{CP}$ = 7.9 Hz, $PCH_2CH_2CH_2$), 30.8 (s, CH_2), 30.4 (s, CH_2), 29.4 (s, CH_2), 28.7 (virtual t, $^1J_{CP}$ = 18.0 Hz, PCH_2), 26.3 (s, PCH_2CH_2); $^{31}P\{^1H\}$ 14.6 (s, $^1J_{PPt}$ = 2576 Hz).[55] IR (cm^{-1}, powder film): $\nu_{C\equiv C}$ 2146 (m), 2003 (w). UV−vis:[56] 275 (76 000), 291 (118 400), 316 (148 800), 352 (9600), 379 (8800), 410 (4800). MS:[57] 1869 (**8**$^+$, 100%), 1791 ([**8**−C_6F_5]$^+$, 2%), 1701 ([**8**−2C_6F_5]$^+$, 6%), no other significant peaks >825.

***trans,trans*-(C_6F_5)($Ph_2P(CH_2)_{12}PPh_2$)Pt($C\equiv C)_4$Pt($Ph_2P(CH_2)_{12}PPh_2$)(C_6F_5) (9).** Complex **2** (0.103 g, 0.050 mmol), CH_2Cl_2 (100 mL), and a solution of $Ph_2P(CH_2)_{12}PPh_2$ (0.065 g, 0.12 mmol)[27,28] in CH_2Cl_2 (120 mL) were combined in a procedure analogous to that for **3**. After 14 h, the solvent was removed by oil pump vacuum. The residue was chromatographed (25 cm silica gel column, 30:70 v/v CH_2Cl_2/hexanes). The solvent was removed from the product-containing fraction by rotary evaporation and oil pump vacuum to give **9** as a yellow solid (0.034 g, 0.018 mmol, 36%), mp >210 °C dec.

NMR (δ, $CDCl_3$) ^1H 7.37 (m, 16H of 8 Ph), 7.28 (m, 8H of 8 Ph), 7.19 (m, 16H of 8 Ph), 2.68 (m, 8H, PCH_2), 2.04 (m, 8H, PCH_2CH_2), 1.56−1.46 (m, 8H, $PCH_2CH_2CH_2$), 1.45−1.23 (m, 24H, remaining CH_2); $^{13}C\{^1H\}$[53,54] 145.7 (dd, $^1J_{CF}$ = 225 Hz, $^2J_{CF}$ = 22 Hz, *o* to Pt), 136.3 (dm, $^1J_{CF}$ = 240 Hz, *m*/*p* to Pt), 132.8 (virtual t, $^2J_{CP}$ = 6.0 Hz, *o* to P), 131.9 (virtual t, $^1J_{CP}$ = 28.0 Hz, *i* to P), 130.2 (s, *p* to P), 127.9 (virtual t, $^3J_{CP}$ = 5.2 Hz, *m* to P), 98.8 (s, PtC≡), 94.8 (s, $^2J_{CPt}$ = 272 Hz,[55] PtC≡*C*), 63.4 (s, PtC≡C*C*), 58.4 (s, PtC≡CC≡*C*), 31.2 (virtual t, $^3J_{CP}$ = 7.2 Hz, $PCH_2CH_2CH_2$), 30.1 (s, $2CH_2$), 28.5 (s, CH_2), 28.4 (virtual t, $^1J_{CP}$ = 18.4 Hz, PCH_2), 25.5 (s, PCH_2CH_2); $^{31}P\{^1H\}$ 13.7 (s, $^1J_{PPt}$ = 2573 Hz).[55] IR (cm^{-1}, powder film): $\nu_{C\equiv C}$ 2142 (m), 1999 (w). MS:[57] 1897 (**9**$^+$, 100%), 1729 ([**9**−C_6F_5]$^+$, 6%).

***trans,trans*-(C_6F_5)($Ph_2P(CH_2)_{18}PPh_2$)Pt($C\equiv C)_6$Pt($Ph_2P(CH_2)_{18}PPh_2$)(C_6F_5) (11).** A Schlenk flask was charged with *trans*,*trans*-(C_6F_5)(*p*-$tol_3P)_2$Pt($C\equiv C)_6$Pt(P*p*-$tol_3)_2$(C_6F_5) (**10**;[13a] 0.105 g, 0.050 mmol) and CH_2Cl_2 (2.0 L). A solution of $Ph_2P(CH_2)_{18}PPh_2$ (0.060 g, 0.106 mmol)[27] in CH_2Cl_2 (10 mL) was added over 5 h. The solution was concentrated by rotary evaporation (100 mL), and ethanol (20 mL) was added. The solution was further concentrated until a yellow powder precipitated (oligomers). The powder was removed by filtration (G3 frit) and washed with ethanol. The filtrate was stored at −18 °C. Yellow needles formed overnight and were collected by filtration, washed with ethanol (5 mL), and dried by oil pump vacuum to give **11**·$(CH_2Cl_2)_{0.67}$ (0.029 g, 0.014 mmol, 27%), mp >230 °C dec. Calcd for $C_{108}H_{112}F_{10}P_4Pt_2$·$(CH_2Cl_2)_{0.67}$: C, 60.13; H, 5.26. Found: C, 59.40; H, 5.25. DSC: desolvation endotherm with T_i, 45.3 °C; T_e, 71.4 °C; T_p, 99.5 °C; T_c, 112.9 °C; T_f, 131.2 °C; exotherm with T_i, 172.9 °C; T_e, 190.9 °C; T_p, 203.1 °C; T_c, 211.8 °C; T_f, 215.2 °C; endotherm with T_i, 215.3 °C; T_e, 227.9 °C; T_p, 241.1 °C; T_c, 246.1 °C; T_f, 246.1 °C.[52] TGA: mass loss 1.9% between 60 °C and 102 °C (calculated for $(CH_2Cl_2)_{0.67}$, 1.7%); onset of further mass loss (T_e), 236.3 °C.

NMR (δ, $CDCl_3$) ^1H 7.38 (m, 16H of 8 Ph), 7.29 (m, 8H of 8 Ph), 7.21 (m, 16H of 8 Ph), 5.28 (s, CH_2Cl_2), 2.69 (m, 8H, PCH_2), 2.08 (m, 8H, PCH_2CH_2), 1.52 (m, 8H, $PCH_2CH_2CH_2$), 1.36 (m, 8H, $PCH_2CH_2CH_2CH_2$), 1.21 (m, 40H, remaining CH_2); $^{13}C\{^1H\}$[53,54] 143.8 (dd, $^1J_{CF}$ = 225 Hz, $^2J_{CF}$ = 30 Hz, *o* to Pt), 136.5 (dm, $^1J_{CF}$ = 242 Hz, *m*/*p* to Pt), 132.8 (virtual t, $^2J_{CP}$ = 6.0 Hz, *o* to P), 131.6 (virtual t, $^1J_{CP}$ = 28.2 Hz, *i* to P), 130.4 (s, *p* to P), 127.9 (virtual t, $^3J_{CP}$ = 5.0 Hz, *m* to P), 103.8 (s, PtC≡), 93.6 (s, PtC≡*C*), 65.0, 62.7, 61.0, 57.3 (4 s, PtC≡C*C*≡*CC*≡*C*), 53.4 (s, CH_2Cl_2), 30.9 (virtual t, $^3J_{CP}$ = 7.9 Hz, $PCH_2CH_2CH_2$), 30.2 (s, CH_2), 30.1 (s, CH_2), 30.0 (s, CH_2), 30.0 (s, CH_2), 28.4 (virtual t, $^1J_{CP}$ = 18.2 Hz, PCH_2), 25.7 (s, PCH_2CH_2); $^{31}P\{^1H\}$ 14.5 (s, $^1J_{PPt}$ = 2554 Hz).[55] IR (cm^{-1}, powder film): $\nu_{C\equiv C}$ 2131 (m), 2092 (s), 1996 (m). UV−vis:[56] 312 (79 200), 331 (233 600), 354 (360 800). MS:[57] 2113 ([**11**−H]$^+$, 100%), 1945 ([**11**−C_6F_5]$^+$, 8%), no other significant peaks >825.

Acknowledgment. We thank the Deutsche Forschungsgemeinschaft (SFB 583), the US NSF (CHE-9732605), Johnson Matthey (platinum loan), the Ministerio de Educación y Ciencia, and the Fulbright Commission (Fellowships, J.M.M.-A.) for support, and Dr. A. M. Arif for one crystal structure.

Supporting Information Available: Details of general methods including cyclic voltammetry, crystallographic data collection and refinement,[58] and associated tables. This material is available free of charge via the Internet at http://pubs.acs.org.

JA0716103